MIKES Metrology

Espoo 2010

ADVANCED APPLICATIONS OF WAVELENGTH TUNABLE LASERS IN METROLOGY AND FUNDAMENTAL PHYSICS

Doctoral Dissertation

Ville Ahtee

Dissertation for the degree of Doctor of Science in Technology to be presented with due permission of the Faculty of Electronics, Communications, and Automation for public examination and debate in Auditorium S1 at the Aalto University School of Science and Technology (Espoo, Finland) on the 19th of November 2010 at 12 noon.

Aalto-yliopisto

ABSTRACT OF DOCTORAL DISSERTATION	
Author Ville Ahtee	
Name of the dissertation Advanced Applications of Wavelength Tunable Lasers in Metrology and Fundamental Physics	
Manuscript submitted 14.6.2010	Manuscript revised 22.10.2010
Date of the defence 19.11.2010	
☐ Monograph	☒ Article dissertation (summary + original articles)

Faculty	Faculty of Electronics, Communications, and Automation
Department	Department of Signal Processing and Acoustics
Field of research	Measurement Science and Technology
Opponent(s)	Dr. Alan Madej, National Research Council of Canada
Supervisor	Prof. Erkki Ikonen
Instructor	Dr. Mikko Merimaa

Abstract

In this thesis, measurement systems based on wavelength tunable lasers have been developed and studied to improve measurement capabilities in the fields of optical metrology and quantum optics.

In the first work presented in this thesis, techniques for precision measurements of absolute spectral irradiance responsivity of detectors were investigated. Two laser-based methods and a traditional monochromator based method were compared in the near infrared wavelength region. The results between absolute responsivity measurements using the three different measurement systems demonstrated agreement at the uncertainty level of less than 0.1 % (k = 1).

The second work consists of an acetylene-stabilized laser and an optical single-frequency synthesizer that were constructed and characterized for precision optical frequency measurements at telecommunication wavelengths. The acetylene-stabilized laser was designed by taking a fiber-based approach, which enabled a relatively straightforward implementation of the optical set-up. The frequency of the stabilized-laser was measured absolutely using an optical frequency comb generator. The results agree well with the recommendation by the International Committee for Weights and Measures (CIPM).

The single-frequency synthesizer was designed for generating a single user-specified frequency from an atomic time base within the 192–196 THz gain bandwidth of an erbium-doped fiber amplifier (EDFA). The synthesizer was utilized for studying spectral lineshapes of acetylene transitions near 1540 nm. The recorded spectra were investigated by theoretical fits and the obtained line-center frequencies were compared to line-center frequencies measured with the acetylene-stabilized laser using the third harmonic technique. The results agreed well with each other.

Final part of the thesis describes a set-up that is capable of emitting indistinguishable single photons using single molecules as photon sources. This was achieved by combining high resolution laser spectroscopy and optical microscopy at cryogenic conditions. Two single molecules in separate microscopes were identified and DC-Stark effect was exploited to shift the resonance frequencies of given molecules for perfect spectral overlap. Excitation by pulsed laser enabled triggered generation of identical single photons from two independent single molecules. The results can be utilized in the development of a number of different quantum information processing schemes.

Keywords	wavelength tunable laser, spectral irradiance, optical frequency measurement, single-photon source		
ISBN (printed)	978-952-5610-63-5	ISSN (printed)	1235-2704
ISBN (pdf)	978-952-5610-64-2	ISSN (pdf)	1797-9730
Language	English	Number of pages	71 p. + appendix 55 p.
Publisher	Centre for Metrology and Accreditation		
Print distribution	Centre for Metrology and Accreditation		
☒ The dissertation can be read at http://lib.tkk.fi/Diss/2010/isbn9789525610642/			

Aalto-yliopisto

VÄITÖSKIRJAN TIIVISTELMÄ	
Tekijä Ville Ahtee	
Väitöskirjan nimi Aallonpituussäädettävien lasereiden pitkälle kehittyneet sovellukset metrologiassa ja perusfysiikan tutkimuksessa	
Käsikirjoituksen päivämäärä 14.6.2010	Korjatun käsikirjoituksen päivämäärä 22.10.2010
Väitöstilaisuuden ajankohta 19.11.2010	
☐ Monografia	☒ Yhdistelmäväitöskirja (yhteenveto + erillisartikkelit)

Tiedekunta	Elektroniikan, tietoliikenteen ja automaation tiedekunta
Laitos	Signaalinkäsittelyn ja akustiikan laitos
Tutkimusala	Mittaustekniikka
Vastaväittäjä(t)	Dr. Alan Madej, National Research Council of Canada
Työn valvoja	Prof. Erkki Ikonen
Työn ohjaaja	TkT Mikko Merimaa

Tiivistelmä

Tässä väitöskirjassa on tutkittu sekä kehitetty aallonpituussäädettäviin lasereihin perustuvia mittausjärjestelmiä ja täten parannettu mittauskyvykkyyttä optisen metrologian ja kvanttioptiikan tieteenaloilla.

Väitöskirjan ensimmäisessä työssä on tutkittu menetelmiä, joita sovelletaan spektrisen irradianssin mittaamiseen käytettävien ilmaisimien herkkyyksien absoluuttiseen määrittämiseen. Tutkittavana oli kaksi laseriin perustuvaa ja yksi perinteinen monokromaattoriin perustuva menetelmä, joita verrattiin toisiinsa lähi-infrapuna-alueen mittauksin. Eri menetelmillä saavutetut mittaustulokset olivat keskenään yhtäpitäviä alle 0,1 %:n epävarmuustasolla (k =1).

Toinen väitöskirjassa esitettävä työ koostuu asetyleenistabiloidun laserin ja optisen yksitaajuussyntetisaattorin kehittämisestä ja karakterisoinnista. Kehitetyt laserjärjestelmät toimivat optisen tietoliikenteen aallonpituusalueella. Asetyleenistabiloitu laser suunniteltiin hyödyntäen optisia kuituja, mikä mahdollisti järjestelmän verrattain suoraviivaisen toteuttamisen. Stabiloidun laserin taajuus mitattiin absoluuttisesti optisen taajuuskamman avulla. Tulokset olivat yhteneviä kansainvälisen mitta- ja painokomitean (CIPM) suositusten kanssa.

Optinen yksitaajuussyntetisaattori suunniteltiin tuottamaan käyttäjän valitsema yksittäinen optinen taajuus atomikellon taajuudesta erbium-seostetun kuituvahvistimen (EDFA) 192–194 THz:n vahvistuskaistalla. Tässä työssä syntetisaattoria käytettiin asetyleenin 1540 nm:n ympäristössä olevien spektriviivojen tutkimiseen. Mitattuihin viivanmuotoihin tehtyjen sovitusten perusteella määritettiin spektriviivojen keskitaajuudet ja näitä verrattiin vastaaviin asetyleenistabiloidulla laserilla kolmannen harmonisen menetelmällä mitattuihin arvoihin. Tulokset olivat keskenään yhtäpitäviä.

Väitöskirjan kolmannessa työssä toteutettiin järjestelmä, jolla voidaan tuottaa yksittäisistä molekyyleistä yksittäisiä, keskenään täysin identtisiä, fotoneja. Järjestelmä toteutettiin yhdistämällä korkearesoluutioinen laserspektroskopia ja mikroskopia kryogeenisissä olosuhteissa. Kahden erillisissä mikroskoopeissa olevan yksittäisen molekyylin resonanssitaajuudet siirrettiin vastaamaan toisiaan DC-Stark-efektiä hyödyntäen. Molekyylien virittäminen pulssitetulla laserilla mahdollisti yksittäisten fotonien samanhetkisen tuottamisen erillisistä molekyyleistä. Työn tuloksia voidaan hyödyntää useissa kvanttilaskentaan ja kvanttitiedonkäsittelyyn tähtäävien järjestelmien kehittämisessä.

Asiasanat	aallonpituussäädettävä laser, spektrinen irradianssi, optisen taajuuden mittaaminen, yksifotonilähde		
ISBN (painettu)	978-952-5610-63-5	ISSN (painettu)	1235-2704
ISBN (pdf)	978-952-5610-64-2	ISSN (pdf)	1797-9730
Kieli	englanti	Sivumäärä	71 s. + liitteet 55 s.
Julkaisija	Mittatekniikan keskus		
Painetun väitöskirjan jakelu	Mittatekniikan keskus		
☒ Luettavissa verkossa osoitteessa http://lib.tkk.fi/Diss/2010/isbn9789525610642/			

Preface

The research work presented in this thesis has been carried out at the Centre for Metrology and Accreditation (MIKES), at the Metrology Research Institute of Helsinki University of Technology (TKK), and at the Laboratory of Physical Chemistry of Swiss Federal Institute of Technology Zurich (ETH) over the years 2005-2008.

I am thankful to my supervisor Professor Erkki Ikonen for the opportunity to work with the research in the interesting field of optical metrology and laser physics, and for giving me the chance to work with so many great people in various institutes during the years spent with this thesis.

I am grateful to my instructor Dr. Mikko Merimaa and Docent Kaj Nyholm for excellent guidance in research at MIKES and during writing process of this thesis. I want to thank Tuomas Hieta for giving me a hand with building up the set-ups and for the refreshing discussions we had while sharing an office. Dr. Heikki Isotalo and Dr. Antti Lassila are thanked for offering the possibility to carry out research at MIKES Metrology.

Dr. Mart Noorma is very much thanked for sharing his knowledge on optical radiometry and guiding me with research in radiation thermometry at TKK and MIKES.

From ETH I would like to thank Professor Vahid Sandoghdar and his group for introducing me to the field of single-molecule spectroscopy and for very nice companionship during my stay at Zurich. Especially, I want to mention Dr. Andreas Walser, Dr. Robert Pfab, Dr. Robert Lettow, Dr. Alois Renn, and Dr. Stephan Götzinger. Thanks for great support and for many moments to remember.

I want to thank Dr. Steven Brown and Dr. Keith Lykke from the National Institute of Standards and Technology (NIST) for collaboration in research with optical radiometry. Steven Brown and his family are especially thanked for great hospitality during my visit at NIST.

The preliminary examiners of the thesis, Dr. Petr Balling and Professor Tapio Niemi, are thanked for their efforts.

The financial support by the Finnish Foundation for Technology Promotion, Magnus Ehrnrooth Foundation, and the Academy of Finland is acknowledged.

Special acknowledgement for their support goes to my wife Anna and to our lovely little daughter, “Peippo”!

Espoo, October 2010

Ville Ahtee

Contents

List of Publications

This thesis consists of an overview and the following publications.

[I] V. Ahtee, S. W. Brown, T. C. Larason, K. R. Lykke, E. Ikonen, and M. Noorma, "Comparison of absolute spectral irradiance responsivity measurement techniques using wavelength-tunable lasers," Appl. Opt. **46**, 4228–4236 (2007).

[II] V. Ahtee, M. Merimaa, and K. Nyholm, "Fiber-based acetylene-stabilized laser," IEEE Trans. Instrum. Meas. **58**, 1211–1217 (2009).

[III] V. Ahtee, M. Merimaa, and K. Nyholm, "Single-frequency synthesis at telecommunication wavelengths," Opt. Express **17**, 4890–4896 (2009).

[IV] V. Ahtee, M. Merimaa, and K. Nyholm, "Precision spectroscopy of acetylene transitions using an optical frequency synthesizer," Opt. Lett. **34**, 2619–2621 (2009).

[V] R. Lettow, V. Ahtee, R. Pfab, A. Renn, E. Ikonen, S. Götzinger, and V. Sandoghdar, "Realization of two Fourier-limited solid-state single-photon sources," Opt. Express **15**, 15842–15847 (2007).

[VI] V. Ahtee, R. Lettow, R. Pfab, A. Renn, E. Ikonen, S. Götzinger, and V. Sandoghdar, "Molecules as sources for indistinguishable single photons," J. Mod. Opt. **56**, 161–166 (2009).

Author's contribution

All publications included in the thesis are results of team work. The author has prepared the manuscripts for Publications I, II, III, and VI.

In the work reported in Publication I the author has been responsible for the measurements done for the comparison at TKK. He has also analyzed all the measurements presented in this publication.

The author has contributed to the design of the measurement set-ups presented in Publication II and III and he has constructed and characterized the set-ups. He has carried out and analyzed all the measurements presented in these publications. In Publication IV the author has carried out all the measurements and made the numerical simulations.

In the work presented in Publications V and VI the author was involved in the planning of the project, constructed the initial measurement set-up and made the first proof-of-the-principle measurements that demonstrated spectrally overlapping two natural lifetime limited single-molecule resonances. He also analyzed the measurements presented in Publication VI.

1 Introduction

1.1 Background

The proposal for the realization of Light Amplification by Stimulated Emission of Radiation (LASER) in 1958 [1] followed by the demonstration of the first lasing device, a ruby laser in 1960 [2], have been one of the most remarkable landmarks in the history of modern science. Not only that the demonstration of the laser action is a great manifestation of the physical phenomena by itself but, above all, it has opened a door for experiments and technological innovations that would have been impossible to carry out using traditional light sources.

Today, lasers have become an everyday tool in research laboratories where fundamental physical phenomena are investigated. They are used, for example, in spectroscopy to probe atomic and molecular structures and hence to obtain information from the interaction between light and matter [3] or to test the theories of modern physics [4]. Also in other fields of science lasers are extensively used. In metrology, lasers are used for the realization of SI units [5]. The meter, for instance, can be realized by the radiation of a frequency-stabilized laser system [6], and the most stable clocks are based on optical transitions in single ions [7,8,9] or neutral atoms in an optical lattice [10] probed by lasers. Another example from the field of metrology is the realization of the unit for luminous intensity, the candela [11], for which detector responsivity calibrations are made using optical power from a laser source at specific wavelengths.

In telecommunication, lasers have enabled long haul optical data transmission [12], which today forms the backbone of the physical layer of the Internet. Other examples of applications based on laser sources range from consumer products to industrial processing tools and state-of-the art medical instruments. In 2008 the estimated total value of global laser market was $7.40 billion [13].

What then makes the laser so special? The answer lies in the mechanism of the photon generation. In classical light sources, the photons are generated by a spontaneous emission process, which produces photons with random phase and direction over a

broad spectral range. The laser operation, in contrary, is based on stimulated emission where the photons generated are exact copies of one another. As the light emitted form a laser is highly coherent, phase is well defined over long distance and coherent phenomena can be used in measurements.

The first operational laser, a ruby laser, was a solid-state laser acting in pulsed mode at 694 nm [2]. Soon after the pulsed ruby laser was introduced, continuous wave (cw) lasing was demonstrated in a gaseous helium neon mixture pumped by electrical discharge [14] providing the first truly coherent light source at 633 nm. Since then, in addition to various solid-state and gas lasers, several other types of laser have been developed, for example, semiconductor lasers [15] and dye lasers [16]. Laser operation on numerous wavelengths over a spectral range from a few nanometers to hundreds of micrometers has been reported [17].

In most cases, the gain of the lasing medium is restricted to a narrow spectral range, which results into a very limited wavelength tuning range. However, some laser types have a broad gain bandwidth and are operable over fairly large wavelength ranges. These include liquid dye lasers [18], solid-state Ti:Sapphire lasers [19], and external-cavity diode lasers (ECDL) [20]. Using frequency mixing processes provided by non-linear optics, e.g., second harmonic generation (SHG) and optical parametric oscillation (OPO), the wavelength range can be further extended. A number of applications benefit from the broad gain bandwidth. For example, in spectroscopy, wide atomic or molecular absorption bands can be recorded by continuous frequency sweeps. Broad gain bandwidth also enables mode-locked operation and generation of wide continuums.

In this work, several measurement systems based on broad wavelength range lasers have been developed and studied to improve measurement capabilities in the field of optical metrology and in quantum optics. The following chapter summarizes the progress of this work.

1.2 Aim and scope of this thesis

In Chapter 2, techniques for precision measurements of spectral irradiance and radiance responsivity of detectors are discussed. Publication I reports results of a work where three different methods for the measurement of the absolute spectral irradiance responsivity were compared and studied. In the study, two laser-based methods and a traditional monochromator based method were compared in the near infrared wavelength region. The aim of the work was to validate the uncertainty level of the laser-based measurement systems developed at the Metrology Research Institute (MRI) of the Helsinki University of Technology (TKK) [21] and at the National Institute of Standards and Technology (NIST) [22]. The work was the first detailed study of different spectral irradiance responsivity measurement methods reported in the near infrared. The results between the different measurement systems demonstrated agreement at the uncertainty level of less than 0.1 % (k = 1).

In Chapter 3 a research work carried out at the MIKES is presented. The work aimed for developing an optical single-frequency synthesizer for precision optical frequency measurements at telecommunication wavelengths near 1.5 µm. To study the feasibility of the scheme based on fiber optics, a fiber-based acetylene-stabilized laser, described in Publication II, was first constructed and characterized. For the first time, standard fiber optic components were utilized almost exclusively in a construction of a frequency-stabilized laser. In the set-up, the light is coupled to free space only to pass through a gas cell, where the Doppler-free spectrum of acetylene is detected. The length of the optical path in the spectroscopy arrangement was dithered with a piezoelectric transducer to average out interference effects. This enabled performing high precision spectroscopy with a fiber-based set-up. The absolute frequency of the laser stabilized to five different transitions of $^{13}C_2H_2$ at ($\nu_1 + \nu_3$) band was measured using an optical frequency comb generator. The results agree well with the recommendation by the International Committee for Weights and Measures (CIPM).

The developed optical single-frequency synthesizer is presented in Publication III. The synthesizer was designed for generating a single user-specified frequency from an

atomic time base within the 192–196 THz gain bandwidth of an erbium-doped fiber amplifier (EDFA). A phase-coherent link between an atomic time base and optical frequencies is established using an optical frequency comb generator. Continuous frequency scanning of the synthesized optical frequency is possible in sub-kilohertz resolution, in principle, over the entire gain bandwidth of the EDFA. The capability of repeating the measurements on the absolute frequency scale and the extremely high intensity stability of the synthesizer allows performing optical frequency measurements at telecommunication wavelengths in unprecedented accuracy. The synthesizer is directly applicable for characterization of optical components used in telecommunication networks or as a frequency reference when calibrating acetylene-stabilized lasers as well as for performing high precision spectroscopy without modulation techniques.

In Publication IV, we reported of a work where the synthesizer was utilized for studying spectral lineshapes of acetylene transitions near 1540 nm. The high signal-to-noise ratio (SNR) of the recorded spectra allowed investigating the lineshapes by theoretical fits and comparing the line-center frequencies to line-center frequencies obtained with a frequency-stabilized laser using the third harmonic technique. Thus, using the synthesizer the effect of line-shape asymmetries and modulation techniques to the lock-point of a frequency-stabilized laser could be studied.

Chapter 4 describes a work done at ETH in the field of quantum optics. The objective of the research was to develop a set-up for demonstrating quantum mechanical two-photon interference using independent single molecules as single-photon sources.

A first step towards the goal is presented in Publication V, where emission of indistinguishable single photons, required for the two-photon interference experiment, was reported. For the first time, two independent solid-state sources were used for producing indistinguishable single photons. In the set-up organic single-molecules in crystalline host matrix were used as sources. The emission of indistinguishable single-photons was achieved by combining high resolution laser spectroscopy and optical microscopy at cryogenic conditions. Wavelength tunable liquid dye lasers were used to excite two individual molecules under two independent microscopes. DC-Stark effect

was exploited to shift the resonance frequencies of given molecules for perfect spectral overlap.

In the further step of the project, reported in Publication VI, a pulsed laser was introduced to the set-up for triggered generation of single photons. For the first time, pulsed excitation was combined with high spectral and spatial resolution in single-molecule spectroscopy. The experimental arrangement set the ground for the realization of a two-photon interference experiment reported recently [23]. The results of this work are important for the development of various quantum information processing schemes utilizing quantum interference.

2 Characterization of absolute spectral irradiance responsivity of detectors using wavelength-tunable lasers

Optical radiometry is a field of science that studies the measurement of energy of the electromagnetic radiation and its propagation in a wavelength range between 5 nm and 100 µm [24]. The quantities of interest are often related to the spectral power distribution of the studied electromagnetic radiation field. Such quantities are, e.g., spectral radiance and irradiance. Radiance is a measure of radiant power through a surface to a specified direction within a given solid angle and has a unit of [$W \cdot m^{-2} \cdot sr^{-1}$]. Irradiance is a measure of radiant power falling on a certain area of a surface and has a unit of [$W \cdot m^{-2}$]. In this thesis, characterization methods of spectral irradiance responsivity of detectors using laser sources have been studied. The motivation for the work was to develop the accuracy of absolute radiation thermometry [25,26,27,28]. In metrology, applications of radiometric temperature measurements include realization of the spectral irradiance scale [29]. In industry, these measurements are needed for monitoring high temperature materials processes. Examples of other applications that benefit from high precision measurements of spectral irradiance include thermal imaging, night vision and solar irradiance measurements.

2.1 Radiometric temperature measurements

Radiometric methods are needed for measurement of high temperatures, for which methods utilizing contact sensors cannot be applied. Traditionally, high temperature measurements have been based on the ratio pyrometry using the Planck radiance law [24]. For an ideal blackbody, the spectral radiance $L(\lambda,T)$ is given by:

$$L(\lambda,T) = \frac{c_1}{\lambda^5\left[\exp(c_2/\lambda T)-1\right]}, \qquad (1)$$

where λ is the wavelength, and T is the temperature, $c_1 = 1.9104282\times10^{-16}\ \mathrm{Wm^2/sr}$ is the first radiation constant, and $c_2 = 1.4387752\times10^{-2}$ mK is the second radiation constant.

Figure 1 shows the spectral radiance of an ideal blackbody, calculated using equation (1), at three different temperatures. The spectral power density at all wavelengths is a monotonic function of temperature, which enables determining the temperature by measuring the radiance on a known wavelength band anywhere on the curve.

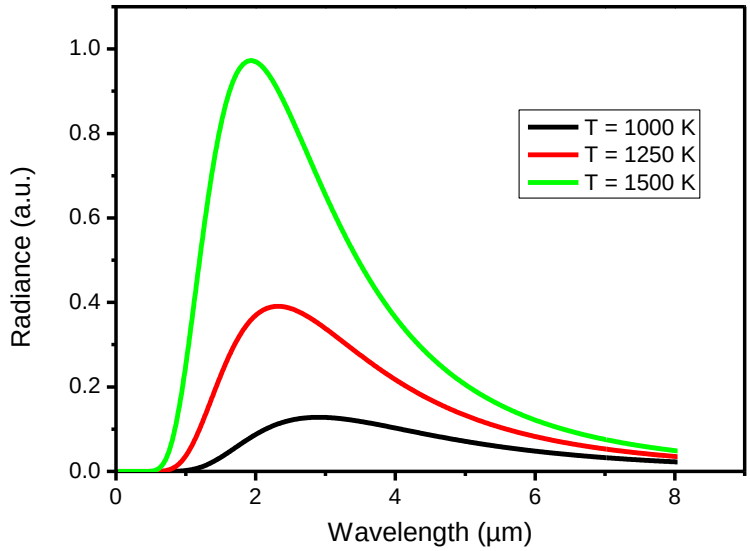

Figure 1. Spectral radiance emitted by an ideal blackbody at three different temperatures.

In the International Temperature Scale of 1990 (ITS-90) [30] the temperatures above the freezing temperature of silver (961.78 °C) are defined in terms of spectral radiance ratios to the silver-, gold- or copper-freezing temperature fixed point blackbody sources. The realization is obtained by relative measurements against one of the fixed points as

$$\frac{L_\lambda(T_{90})}{L_\lambda[T_{90}(X)]} = \frac{\exp\left\{c_2\left[\lambda T_{90}(X)\right]^{-1}\right\}-1}{\exp\left\{c_2\left[\lambda T_{90}\right]^{-1}\right\}-1}, \qquad (2)$$

where $T_{90}(X)$ is the temperature of any one of the silver-, gold-, or copper-freezing points, $L_\lambda(T_{90})$ and $L_\lambda[T_{90}(X)]$ are the spectral radiances emitted by a blackbody at the wavelength λ at T_{90} and at $T_{90}(X)$, respectively.

In the ITS-90, the assigned temperatures for the Ag, Au, and Cu freezing points, result from thermometry using ratio pyrometry referenced to constant-volume gas thermometry (CVGT) measurements at lower temperatures [31]. The thermodynamic

temperature uncertainties of these fixed points arise primarily from the uncertainties in the lower temperature gas thermometry.

The uncertainty of a temperature measurement of higher temperature blackbodies referenced to the fixed points can be estimated by applying Wien's approximation [24]

$$L(\lambda,T) = \frac{c_1}{\lambda^5\left[\exp(c_2/\lambda T)\right]}. \tag{3}$$

From the derivative of $L(\lambda,T)$ with respect to temperature

$$\frac{dL(\lambda,T)}{dT} = \frac{c_1 c_2}{\lambda^6 T^2\left[\exp(c_2/\lambda T)\right]}, \tag{4}$$

it follows that

$$\frac{\Delta L}{L} = \frac{c_2}{\lambda}\frac{\Delta T}{T^2}, \tag{5}$$

which relates the changes in L with the changes in T. When combined with equation (2) this shows that the temperature uncertainty of an ITS-90 assigned blackbody, $u(T_{BB})$, increases as the square of the temperature ratio:

$$u(T_{BB}) = u(T_{FP})\left(\frac{T_{BB}}{T_{FP}}\right)^2, \tag{6}$$

where T_{FP} and $u(T_{FP})$ are the temperature and the uncertainty of the fixed point blackbody and T_{BB} is the temperature of the higher temperature blackbody.

Using absolutely characterized filter radiometers or pyrometers to measure the spectral radiance or irradiance, the thermodynamic temperature of a blackbody can be determined directly and the uncertainty at high temperatures can be reduced [32]. Such detector based methods were long limited by capability of measuring absolute radiation power. The introduction and further development of cryogenic radiometers [33,34] has offered a direct link between optical power and electrical units. This has significantly decreased uncertainties associated to optical power measurements and has made the detector-based absolute radiometric temperature measurements feasible.

2.1.1 Sources of uncertainty

The major sources of uncertainty in the detector-based radiation temperature measurement arise from the spectral responsivity characterization of the detector. In addition to uncertainty in optical power, the wavelength uncertainty is often also a major component in the uncertainty budget. Figure 2 shows radiance of a gold point blackbody source together with responsivity curve of a near infrared filter radiometer that is typically used for radiometric temperature measurements at TKK. Figure 2 shows that as the radiance of the source is highly wavelength dependent on the measurement band, accurate wavelength determination of the detector's responsivity is essential. Also, the out-of-band attenuation of a narrow-band detector has to be well known as the total amount of optical power at the long-wavelength end is significant and the power coupled to the detector cannot be neglected.

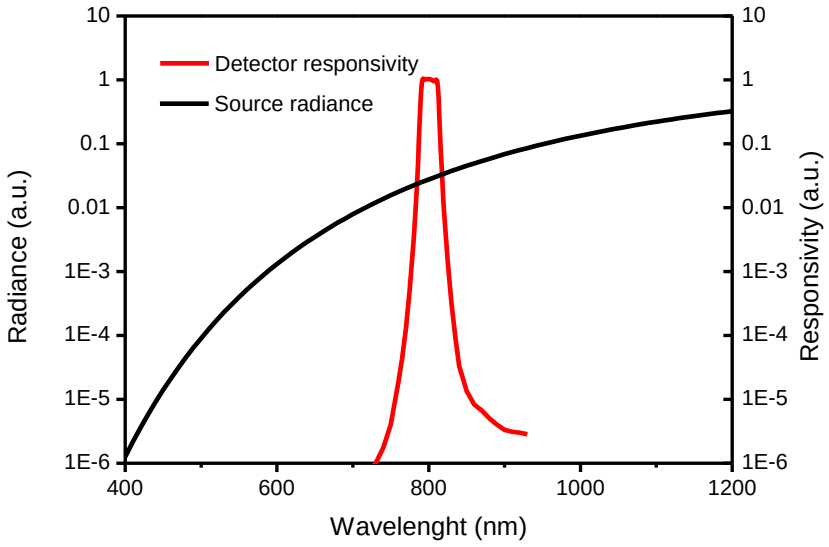

Figure 2. Spectral radiance of a gold point blackbody (T = 1064.18 °C) shown together with the responsivity of a narrow-band near infrared filter radiometer.

2.2 Spectral irradiance responsivity measurement techniques

Traditionally the spectral irradiance responsivity of a detector has been calibrated using a lamp and a monochromator as a radiation source [35,36]. This approach is convenient as broad spectral range can be covered using one source and calibration can be

performed rapidly. However, the achievable uncertainty is often limited by the low radiant flux and the relatively broad spectrum of the source. The low radiant flux limits measurements especially at the out-of-band regions. Broad spectral width, on the other hand, limits the accuracy of determining the responsivity as a function of the wavelength due to convolution effects, especially, at steep transition bands of the device under study.

Using single-mode wavelength tunable dye and Ti:Sapphire lasers, whose output powers range from a few hundred milliwatts up to several watts, the wavelength range from 450 nm to 1100 nm can be continuously covered. Using nonlinear optics this wavelength range can be readily extended, albeit at lower optical power. By stabilizing the laser intensity, relative intensity variations can be reduced below 0.01 %. An active control of the laser cavity and the use of wavelength selective elements provide stable operation in a single longitudinal mode with less than 1-MHz linewidth. These properties make laser sources an attractive alternative for calibrations of detectors [21,22,37]. Indeed, when using wavelength tunable lasers instead of a lamp and a monochromator, the limitations of the traditional calibration methods can be overcome. However, because of the high spatial and temporal coherence of the laser sources, care has to be taken to avoid errors due to interference effects inside the device under test [21, Publication I].

One way to circumvent the interference effect could be to use a pulsed laser instead of a cw source [38]. A Gaussian pulse with duration of a few tens of picoseconds would lead to a linewidth of approximately 100 GHz, which could be utilized in fringe reduction through averaging. However, the center wavelength of spectrally wide pulsed radiation cannot be controlled or measured as accurately as the center wavelength of a narrow cw source. Also, care has to be taken not to saturate a detector under study with high peak power pulses.

Another recently studied approach is provided by supercontinuum laser sources [39], where spectrally broad radiation is generated using a pulsed laser and a photonic crystal fiber (PCF). A supercontinuum source could replace a lamp as a monochromator’s light source providing orders of magnitude increased spectral power densities. As the

radiation from a fiber source can easily be focused into small spot size, the radiation can be coupled into a monochromator using a small entrance slit. This would enable both high spectral resolution and high spectral power density at the monochromator's output.

2.2.1 Comparison of laser-based calibration methods at TKK and NIST

In this work, two laser-based spectral irradiance responsivity characterization methods were comparatively studied in the near infrared range. The studied measurement systems were the laser scanning facility (LSF) [21] at TKK and the facility for Spectral Irradiance and Radiance responsivity Calibrations using Uniform Sources (SIRCUS) [22] at NIST. The laser-based methods were compared also to a conventional lamp and a monochromator based method. Earlier comparisons of different calibration methods of spectral irradiance responsivity have revealed deviations which have exceeded the stated uncertainties [40,41]. One reason for these discrepancies has been reported to be due higher than expected uncertainties in the wavelength scales at the comparison laboratories [41]. From this point of view, the laser-based calibration methods are likely to be more exact because of the narrow linewidth of the laser radiation and the ability for accurate real-time wavelength monitoring.

The construction of the filter radiometer used in this work as a measurement artifact is shown in Figure 3. It consists of a precision aperture with a nominal diameter of 3 mm, a band-pass interference filter with a bandwidth of 24 nm (full width at half maximum, FWHM), and a three-element silicon trap detector [42]. The temperature of the aperture and the filter are stabilized during measurements to (25 ± 0.5) ºC.

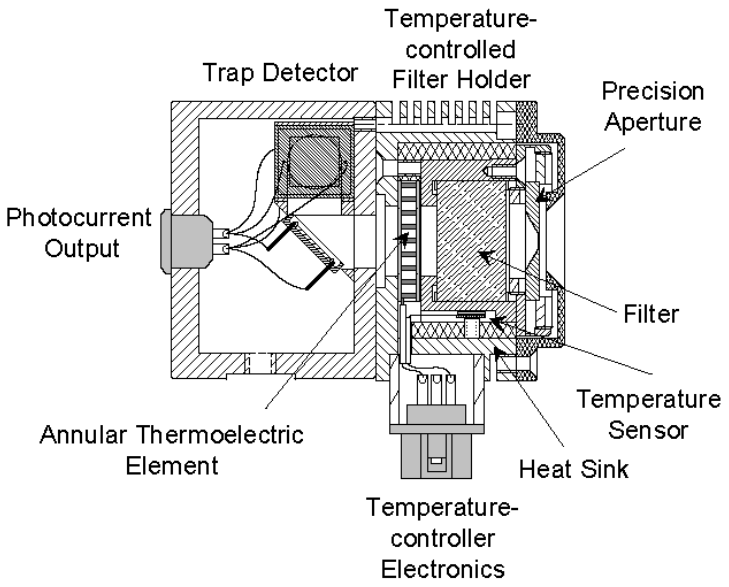

Figure 3. The construction of a typical filter radiometer used in TKK. Figure reproduced from Ref. [41].

Description of the laser-based measurement systems

The studied measurement set-ups have completely independent traceability chains from two independent primary standard cryogenic radiometers. Wavelength-tunable Ti:Sapphire lasers are used at both laser-based set-ups as the light sources and calibrated silicon trap detectors as the reference standards for spectral power responsivity. At TKK the trap detector calibration is based on optical power responsivity measurements at three visible laser wavelengths with a cryogenic radiometer. The responsivity is modeled up 1150 nm. At NIST the reference detector is calibrated directly against national primary standards for spectral power responsivity [34].

The method to generate a uniform monochromatic irradiance is completely different between the two set-ups. SIRCUS at NIST uses an integrating sphere to generate a uniform irradiance field, while LSF at TKK is based on the raster scanning a single collimated laser beam relative to a device under test [43]. The irradiance responsivity on LSF measurement is calculated by summing the resulting photocurrent I at each point, multiplying by the step sizes, and dividing by the incident power P_L as

$$S(\lambda) = \frac{\sum_{j=1}^{n_x} \sum_{k=1}^{n_y} I_{j,k} \Delta x \Delta y}{P_L}. \qquad (7)$$

In equation (7), n_x and n_y are the numbers of measurement points in horizontal and vertical directions, Δx and Δy are the horizontal and vertical distances between the measurement points.

The measurements made with the two laser based set-ups were compared to a measurement made on the monochromator based Visible to Near-Infrared Spectral Comparator Facility (SCF) [35] at NIST, which utilizes a 100 W quartz halogen lamp as a light source. The measurements were done using 4-nm bandwidth. In the SCF the measurement principle is also based on raster scanning the monochromator's output beam.

Interference effects

As explained above, interference effects have to be taken into account when lasers are used in spectral responsivity calibrations. The interference can be minimized by proper coatings on optical surfaces and by using a suitable geometry. In this measurement, for example, the filter of the detector was antireflection coated and the filter surfaces were slightly wedged. However, an interference pattern with 0.2 nm period and 0.5 % peak-to-peak amplitude is still present.

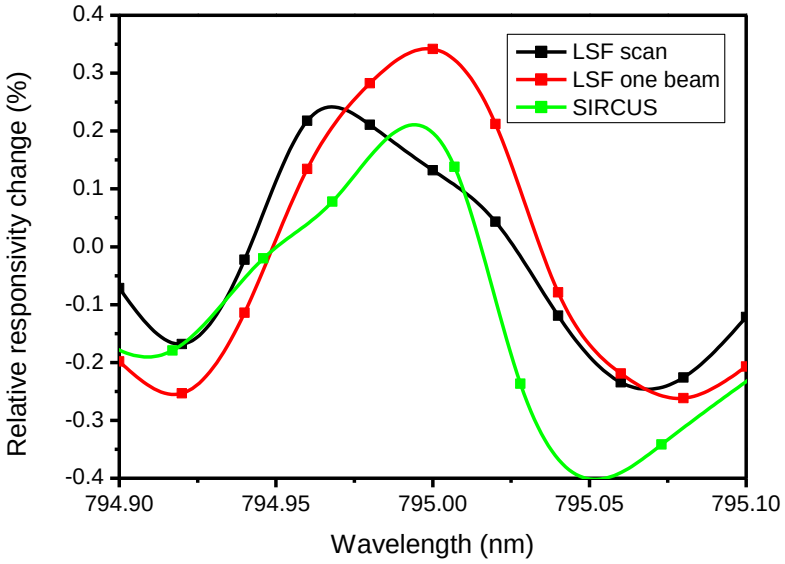

Figure 4. Interference pattern on the filter radiometer's responsivity measured close to 795 nm on SIRCUS, LSF, and with single beam technique on LSF [Publication I].

On SIRCUS calibration the effect of interference was taken into account by taking measurements with 0.02 nm intervals on average, which enabled determination of the true responsivity curve. On LSF, where the scanning method limits the practical number of measurement points, a correction was made to every measurement point. This was done by measuring a relative responsivity of the detector over an oscillation cycle around an absolute raster scanned measurement point using a single beam at the center of the aperture. Based on the single beam measurements, the absolute responsivity was corrected to correspond to the average of the interference pattern. The applicability of the single beam method was confirmed by measuring a period of an oscillation pattern with single beam and raster scanning techniques. The result of this measurement is shown in Figure 4 together with a SIRCUS measurement.

Results of the comparison

Figure 5 shows the results of the measurements performed with the three set-ups. The irradiance responsivity measurements obtained with the two laser-based methods have an excellent agreement. The shape of the responsivity curve obtained from the

measurements on SCF is highly affected by the large bandwidth of the source, which makes the individual measurement points to represent values that are spectrally averaged over several nanometers.

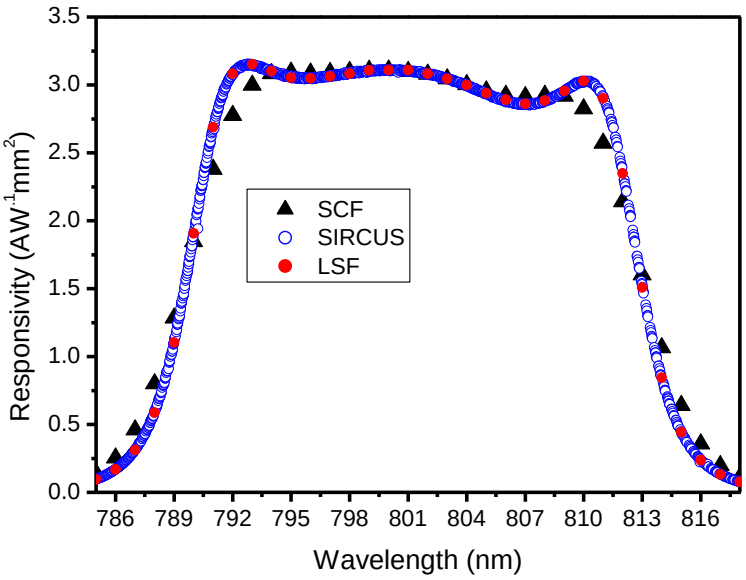

Figure 5. Spectral irradiance responsivity of the near infrared filter radiometer measured on SIRCUS, LSF, and SCF [Publication I].

To quantitatively compare the measured data, the integrated irradiance responsivity and the effective wavelength were calculated. The results are shown in the Table I as relative differences to the weighted average of all three methods together with the stated standard uncertainties for each set-up. The weighted averages were calculated as

$$\bar{x} = \frac{\sum_{i=1}^{3} x_i u_i^{-2}}{\sum_{i=1}^{3} u_i^{-2}}, \qquad (8)$$

where x_i are the calculated integrated responses/effective wavelengths obtained with each method and u_i are the corresponding standard uncertainties.

It should be noted that the effective wavelength in SCF measurements is affected by the convolution effect due 4-nm source linewidth. The effect was estimated to be approximately 0.01 nm.

Table I. Integrated responses and effective wavelengths obtained on each set-up as compared to weighted average of the three measurements. Results are calculated from the measurement data over 785 - 818 nm range. The corresponding standard uncertainties are shown.

	Integrated irradiance responsivity		Effective wavelength	
	Relative difference to weighted average × 10^{-4}	Relative standard uncertainty × 10^{-4}	Difference to weighted average [nm]	Standard uncertainty [nm]
SIRCUS	-1.0	5.2	0.001	0.001
LSF	3.0	8.9	-0.006	0.003
SCF	-0.6	59	0.016	0.1

All three methods agree well with each other in terms of the integrated responsivities; the laser-based methods offering significantly lower uncertainties than the monochromator-based method. The calculated effective wavelength values on SIRCUS and LSF measurements match well with each other, within expanded (k = 2) uncertainties. Also, the effective wavelength extracted from the SCF agrees well with the average of all three methods, although the uncertainty is much higher.

The results of this comparison have implications for a number of radiometric applications where high-accuracy spectral radiance and irradiance measurements are crucial. For instance, the uncertainty in an absolute detector-based radiometric temperature scale depends mostly on the accuracy of the spectral radiance and irradiance responsivity scales. Freezing temperatures of gold, silver, and aluminum fixed points, defined by ITS-90, have been measured using radiometric detectors traceable to absolute cryogenic radiometers, with uncertainties similar to the thermodynamic measurements of temperature reported in the ITS-90. For example, such a measurement was conducted using the filter radiometer characterized in this work in a study where thermodynamic temperatures of blackbody radiators were measured at MIKES [28]. The thermodynamic temperature measurement of a silver fixed-point cell using the filter radiometer gave excellent agreement with the ITS-90 determined temperature (961.78 °C), the deviation being only 0.05 K with standard uncertainty of 0.109 K.

The results of this comparison may also have implications in photometry where tunable lasers can be utilized to measure the spectral responsivity of photometers with low uncertainty. In such measurements the advantage of using lasers arises primarily because of the improved accuracy of the wavelength scale.

3 Precision optical frequency measurements at telecommunication wavelengths

Frequency can be measured at the lowest uncertainty of all physical quantities. This applies also at the optical domain where the most accurate atomic clocks operate today [7,8,9,10], although the definition of the second is still tied to the ground state hyperfine splitting of Cesium at microwave region. Past measurements of optical frequencies have led to a number of technological breakthroughs, one of the most significant being the current definition of the meter adopted by General Conference on Weights and Measures (CGPM) in 1983 [44]: "The Meter is the length of the path traveled by light in vacuum in 1/299792458 of a second." This definition fixes the speed of light and relates the SI-base unit of length, the meter, with that of the time, the second.

3.1 Absolute measurement of optical frequency

A measurement is absolute when it is referenced to the definition of the appropriate SI unit(s). An absolute frequency measurement must be based on the time unit second and thus referenced to a Cs-clock. The measurement of optical frequency at hundreds of terahertz is anything but trivial. Direct frequency counting using electronic circuits is limited to frequencies up to a few tens of gigahertz. Thus, to measure visible optical frequencies a method to cover orders of magnitude wide frequency gap between an atomic time base and optical frequencies is needed. Until last decade, this was one of the trickiest challenges in metrology and diverse techniques to do this were investigated.

3.1.1 Traditional approach

Optical frequencies were first absolutely measured in the beginning of 1970's using synthesis by harmonics approach to construct a frequency chain [45,46,47,48,49,50]. Although the frequency chains were the only viable option at that time, the limitations of such systems were obvious. The complexity of the approach required resources that were available only at a few major metrology institutes and the chain had to be designed

to measure a particular frequency. Also, the multiplication of phase noise with harmonic synthesis limited the performance of frequency chains. Nevertheless, successful measurement of an iodine-stabilized He-Ne laser at 633 nm in 1982 led to re-definition of the meter.

In 1990's optical frequency measurement methods based on difference-frequency syntheses were developed. Probably the most notable of these techniques was frequency interval bisection [51], which relied on subdividing a frequency gap between two optical frequencies (f_1 and f_2) by phase locking a third frequency f_3 to the exact average of the frequencies f_1 and f_2. In principle, concatenation of approximately 12 bisection stages links visible optical frequencies to microwave region.

3.1.2 Full octave optical frequency comb technique

Advances in mode-locked laser technology in the end of 1990's provided ever wider measurement ranges [52] and paved a way for a quantum leap in the measurement of optical frequencies. At the turn of millennium the introduction of a full-octave optical frequency comb generator revolutionized the field of optical frequency metrology by providing direct phase coherent link between optical and microwave frequencies [53,54,55]. Using a Ti:Sapphire femtosecond mode-locked laser and a photonic crystal fiber (PCF) [56], a dense comb of equally spaced frequencies spanning over an optical octave was produced. The comb could be directly stabilized to a microwave standard giving each frequency component an absolutely known value. This enabled practical absolute measurements of any optical frequency over the entire visible spectrum extending to near infrared. Soon after, an octave spanning comb spectrum at near infrared was demonstrated using an erbium-doped fiber laser [57,58].

In this work, a Ti:Sapphire frequency comb generator has been utilized to measure the absolute frequency of the constructed acetylene-stabilized laser and for optical single-frequency synthesis at near infrared. In the next section, the operating principle of a full octave optical frequency comb generator is briefly reviewed.

3.1.3 Ti:Sapphire femtosecond laser comb

Operation of a conventional full octave spanning optical frequency comb generator is typically based on a mode-locked laser, which produce pulses whose duration is in the femtosecond scale with a repetition rate in between 100 MHz and 1 GHz. By Fourier transforming such a pulse train from time domain to frequency domain, it is seen that the result is a comb like structure of evenly spaced frequency components [59].

The spacing between the frequency components is directly given by the repetition rate (f_{rep}) of the pulsed laser. The location of each frequency component is, however, not an integer number times the repetition rate. This is due to the fact that the group and phase velocities differ inside the laser cavity and the center of envelope with respect to carrier changes from pulse to pulse. In frequency domain, this phenomenon causes an offset frequency for the frequency comb structure, commonly referred as the carrier-envelope-offset (CEO).

The spectral width of the output of a femtosecond laser is determined by the duration of the emitted pulses. The width of the spectrum resulting from Gaussian shaped pulses with duration of 30 fs is approximately 15 THz (FWHM). To broaden the spectrum, the pulse train from the laser is taken through a PCF. The size of the core and the dispersion properties of a PCF can be tailored for efficient pulse compression in the fiber. The resulting self-phase modulation (SPM) and other non-linear effects broaden the spectrum [60] and at the fiber output a spectrum spanning over an octave in frequency can be obtained. It has also been demonstrated that octave-spanning spectra can be achieved directly from a Ti:Sapphire laser using double-chirped mirrors and a second intracavity focus in a glass plate for additional SPM effects [61].

In order to generate a comb of absolutely known optical frequencies, the repetition rate and the CEO frequency have to be phase-locked to an atomic time base. A hydrogen maser [62] is very desirable reference clock as it has excellent short- and long-term stability and it can be tuned with high precision to match the frequency distributed by the Cs-clock. When the repetition rate and the CEO frequency are stabilized, the frequency of every comb component can directly be calculated as

$$f_n = nf_{rep} \pm f_{CEO}, \quad (9)$$

where n is the number of the comb component and f_{CEO} is the carrier-envelope-offset frequency.

Stabilization of the repetition rate is relatively straightforward as it can be directly measured at the output of the femtosecond laser using a high speed photodetector and synchronized to a microwave source using an analog mixer, loop-filter, and a piezoelectric transducer (PZT) to control the cavity length.

In contrast to the repetition rate stabilization, the stabilization of the CEO frequency is not trivial because the offset cannot be accessed directly. The possibility to broaden the spectrum over an optical octave allows an elegant method, self-referencing, to be used to solve this problem. In self-referencing, shown schematically in Figure 6, the red end of the comb spectrum is frequency doubled, thus frequency doubling also the CEO frequency. When the frequency-doubled part of the comb spectrum is overlapped with the blue end of the original comb spectrum, having original offset, the resulting beat-note is exactly equal to the CEO frequency, which can then be stabilized using a PLL controlling the cavity dispersion. This can locally be done by adjusting the power of the pump laser. The complication of this method is that obtaining a proper beat signal requires that the frequencies contributing to the signal in corresponding pulses must overlap both spectrally and temporally at high precision. As the signal path contains a number of non-linear and dispersive components, slight deviations in laser parameters and in coupling to the PCF may have dramatic effect to SNR of the measured offset frequency. However, careful control of vibrations and temperature stabilization in addition to active control of the PCF in the coupling provides continuous operation exceeding hours.

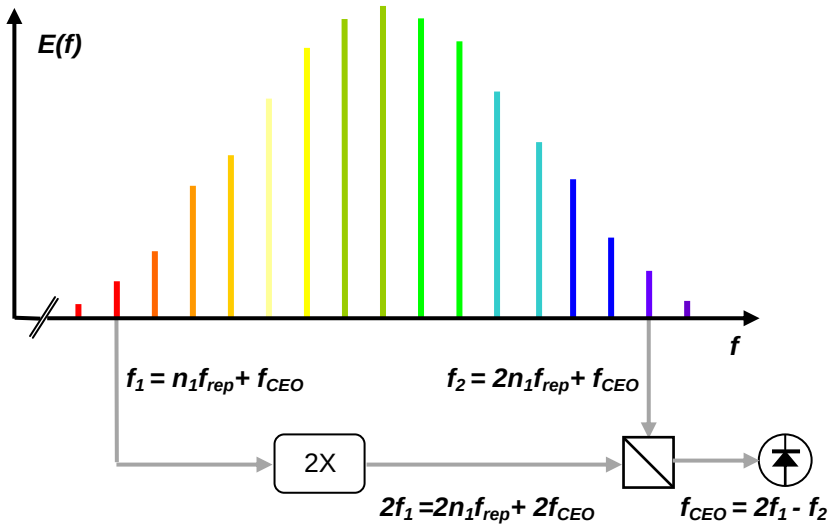

Figure 6. Schematical illustration of self-referencing technique used for measuring the CEO frequency.

3.2 Optical frequency standards

Schemes of using the laser frequency stabilized on an atomic or molecular transition as a wavelength standard have been explored since late 1960's [63] and in 1983 stabilized lasers superseded ^{86}Kr discharge lamps as working wavelength standards. The International Bureau of Weights and Measures (BIPM) maintains a list of radiations recommended by the CIPM for the realization of the definition of the meter as well as for other optical frequency standards covering the wavelength range from 200 nm to 10 µm [6]. A conventional and highly successful method for laser stabilization utilizes saturation absorption spectroscopy [64] and the third harmonic-locking method [65,66] with gas cells. Relative stabilities below 1×10^{-13} at 1 s averaging time can readily be achieved with these systems [67].

An ultimate frequency-stabilized laser is an optical atomic clock. The most stable clocks are based on nearly forbidden transitions in single ions [7,8,9] or in neutral atoms trapped to an optical lattice [10]. The instability of an atomic clock arising from quantum projection noise as a function of the averaging time τ is [68]

$$\sigma(\tau) = \frac{\Delta\nu}{\nu_0}\sqrt{\frac{T}{N\tau}}, \qquad (10)$$

where ν_0 is the transition frequency, $\Delta\nu$ the linewidth, T the cycle time, and N the number of atoms. As the electronic transitions of atoms or ions at visible or near infrared have approximately five orders of magnitude higher frequency compared to a ground state hyperfine structure transition, the fractional uncertainty and instability of an optical clock are potentially extremely small. The utilization of an optical frequency comb generator in reverse direction has enabled transferring the stability of optical frequency references to the microwave region and comparison of different optical clocks. The best optical clocks demonstrate fractional uncertainties less than 10^{-17} [9], which is more than an order of magnitude better than obtained with the best Cs-clocks.

3.2.1 Laser stabilization using gas-cell absorbers

Lasers frequency-stabilized on an atomic or a molecular transition using a gas-cell absorber are widely used, for example, in calibration of lasers used in interferometric length measurements [67,69,70] and in calibration of measurement instruments used in development and maintenance of optical telecommunication networks [Publication II, 71,72,73].

Although absolute optical frequency measurements using frequency combs are now used everyday in today's optical frequency metrology laboratories and ultra precise optical clocks are emerging, the set-ups are still far from simple and are not practical enough to be used as routine working standard calibrations. Thus, development of compact and practical frequency-stabilized lasers is still useful.

As shown by equation (10) the obtainable stability of a stabilized-laser depends inherently on the frequency resolution of such a system, i.e., on the relation of the observed linewidth to the center frequency of the line. A direct measurement of the width of a molecular line in gaseous phase is limited by Doppler-broadening [3]. This inhomogeneous broadening arises from the Doppler-effect and thermal velocity distribution of the molecules leading to a linewidth in the gigahertz range, which is several orders of magnitude higher compared to the natural linewidth of the molecular lines.

A common method to observe Doppler-free spectra is to use saturation spectroscopy, in which counter-propagating pump and probe beam are used for velocity group selection. Pump beam saturates the molecules while the probe beam is used to measure the absorption. When the laser frequency is swept over a molecular line, the spectrally narrow pump and probe beams generally interact with molecules belonging to different velocity groups. However, when the frequency is tuned close to the centre of the line both beams interact with molecules whose velocity components are essentially zero in the direction of the beams. In such conditions the absorption measured by the probe is reduced due to the saturation of the molecules by the pump. This so called Lamb dip [74] ideally shows the natural Lorentzian line shape of the molecule. The excited-state lifetimes of ro-vibrational transitions in molecules can have long lifetimes leading to natural linewidths below the technical broadening mechanism of the spectroscopic system. In such a case, effects like laser linewidth, pressure broadening, or transit time broadening [3] determine the observable linewidth. Nevertheless, it is usually possible to achieve linewidth in the order of one megahertz or below.

A powerful and well known method for stabilizing a laser to an atomic or a molecular line uses frequency modulated measurement and phase sensitive detection (PSD). When the third harmonic of the modulation frequency is detected, the Doppler broadened background is effectively cancelled and the laser can be locked to the steep zero crossing indicating the line center frequency. In addition, the modulation transfers the measurement away from DC-region where 1/*f*-noise dominates and the noise bandwidth can be optimized at detection. This is useful as the detected signals can be small and almost covered by noise. Figure 7 shows typical third-harmonic signal when a modulated laser frequency is tuned over a Doppler-free molecular line.

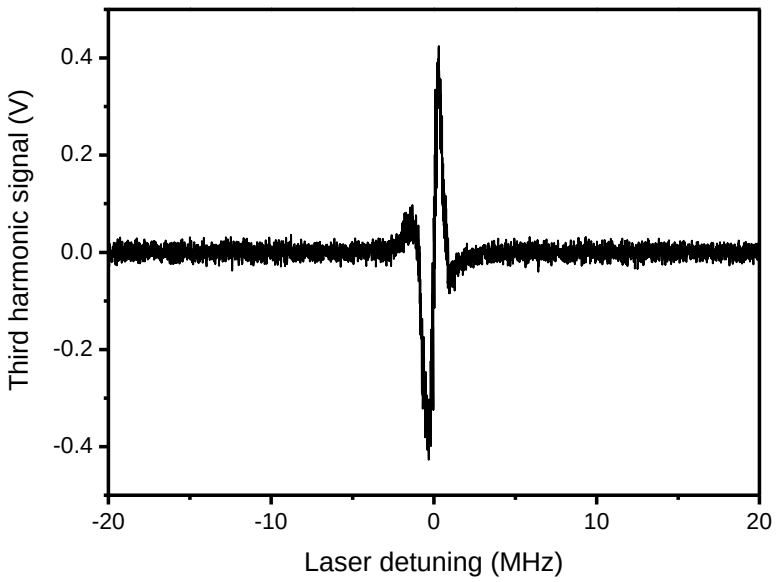

Figure 7. Third-harmonic signal recorded in a measurement where the laser frequency was tuned over a Doppler-free acetylene line. The laser was modulated at 2.94 kHz with a modulation amplitude of (1.0 ± 0.2) MHz peak-to-peak. Sample time was 3 ms [Publication II].

3.2.2 Optical single-frequency synthesizers

An absolute optical frequency reference with a user-specified frequency can be realized with an optical single-frequency synthesizer. In such a device, a single optical frequency is generated with a cw laser, whose frequency is phase-locked to an optical frequency comb referenced to an atomic time base. By proper design of the servo loops, the frequency stability of the synthesizer follows that of the microwave frequency reference.

In addition to frequency metrology, applications in spectroscopy benefit from an absolutely known monochromatic light source. While frequency combs can be used directly for spectroscopy [75,76], the low optical power in each comb component limits the signal-to-noise ratio of the measurements and the techniques needed to extract individual frequency components from the dense comb structure complicate the measurement set-ups. Recently, the development of optical single-frequency

synthesizers have gained much interest in metrology institutes [Publication III,77,78,79,80].

Generally, the structure of an optical single-frequency synthesizer resembles that of some microwave synthesizers. The frequency of a reference oscillator is transferred to a higher frequency using a frequency comb generator and a voltage controlled oscillator is phase-locked to a predetermined comb component. In an optical single-frequency synthesizer, a self-referenced optical frequency comb generator is used and the voltage controlled oscillator is replaced by a tunable cw laser. The phase lock between the cw laser and the optical frequency comb can be established either by optical injection [79,81] or by using an electronic phase-locked loop [Publication III,77,80]. Frequency tuning of the synthesized frequency has been demonstrated by several different methods. One method is to use a fixed frequency comb and by external locking circuits control the beat note between the cw laser and the frequency comb [77] or the output of the cw laser can be shifted by an electro-optical modulator (EOM) [82]. Another approach for sweeping the synthesized frequency is to adjust the frequency comb. This can be accomplished by tuning the repetition rate of the frequency comb [Publication III,80,83]. If the repetition rate is tuned by df then the n^{th} comb tooth and the frequency of the cw laser locked to this component is tuned by $n \cdot df$.

The optical single-frequency synthesizer offers an interesting tool to explore the line shapes of atomic and molecular transitions at high precision. The main advantage of a single-frequency synthesizer is the accuracy and the repeatability of the synthesized frequency. The synthesized frequency is produced at the fractional uncertainty of the microwave reference, which enables long measurement times and averaging over large number of similar measurements. Thus, it is possible to measure a line shape profile with superior signal-to-noise ratio. When a theoretical line profile is fitted to the results, the absolute line center frequency can be determined with low uncertainty. Such measurements are useful in investigations of frequency shifts in lasers stabilized on atomic or molecular transitions. In particular, one of the major sources of uncertainty in frequency stabilized lasers utilizing the third-harmonic technique is the frequency shift

due to modulation, which arises from asymmetry of the observed line. Using a single-frequency synthesizer, insight to the origin of the asymmetry can be obtained.

3.3 Experimental set-ups

In this thesis, two experimental set-ups for precision optical frequency measurements at near infrared telecommunication wavelengths are described. The goal of the work was to construct and characterize a tunable optical single-frequency synthesizer suitable for precision characterization of optical components used in telecommunication networks. To study the feasibility of a fiber-based approach to be utilized on the construction of the single-frequency synthesizer, we first constructed and characterized a fiber-based acetylene-stabilized laser [Publication II]. The absolute frequency of the acetylene-stabilized laser was measured using an optical frequency comb generator. Next, exploiting the results obtained with the acetylene-stabilized laser we re-configured the set-up and constructed the optical single-frequency synthesizer [Publication III]. The optical part of the set-up was essentially the same between the two set-ups. However, instead of locking the frequency of the laser to acetylene lines, we utilized a phase-locked loop to synchronize the laser to an atomic time base via the optical frequency comb generator. We measured spectral lineshapes of acetylene transitions with the synthesizer using unmodulated optical frequency [Publication IV]. In the next chapter the experimental work is described.

3.3.1 Acetylene-stabilized laser

The realization of the acetylene-stabilized laser is based on a commercial fiber coupled external cavity diode laser (ECDL, Photonetics Tunics-PRI) and standard fiber optic components commonly available for the telecommunication wavelengths. In the set-up, the light is coupled to free space only to pass through a 50 cm long acetylene cell at 2.8 Pa pressure. Spectroscopy is performed utilizing saturated absorption in a counter-propagating pump-probe beam configuration. To cancel frequency shifts related to

interference arising from reflections at fiber ends, the length of the optical path in the spectroscopy arrangement was dithered using a piezoelectric transducer (PZT) attached to the end mirror behind the gas cell. This technique has previously been demonstrated in spectroscopy with multi-pass absorption cells [84]. Here the technique was utilized with frequency-stabilized lasers for the first time. To effectively average the interference signal the dithering frequency (125.1 Hz) and amplitude of the mirror (3.1 μm), the modulation frequency of the laser (2.94 KHz), and the time constant of the lock-in amplifier (3 ms) were selected in such a way that the signal arising from dithered interference was sufficiently averaged, while the time constant was still short enough for frequency stabilization. The dithering frequency was synchronized to the modulation frequency and their ratio was chosen to be exactly a half-integer to avoid shifting the harmonics of the dither-frequency to the detection band of the lock-in amplifier. The amplitude of the mirror dither was chosen to be an integer number of half wavelengths of the laser radiation, thus diminishing the residual interference, which scales as inverse to the number of interference cycles averaged. Figure 8 demonstrates the effect of the mirror-dither technique on a laser frequency sweep over P(16) line of ($\nu_1 + \nu_3$) band of $^{13}C_2H_2$ recorded from the low-pass filtered output of the photodiode amplifier used for detection. The optical power used in the experiment was 100 mW.

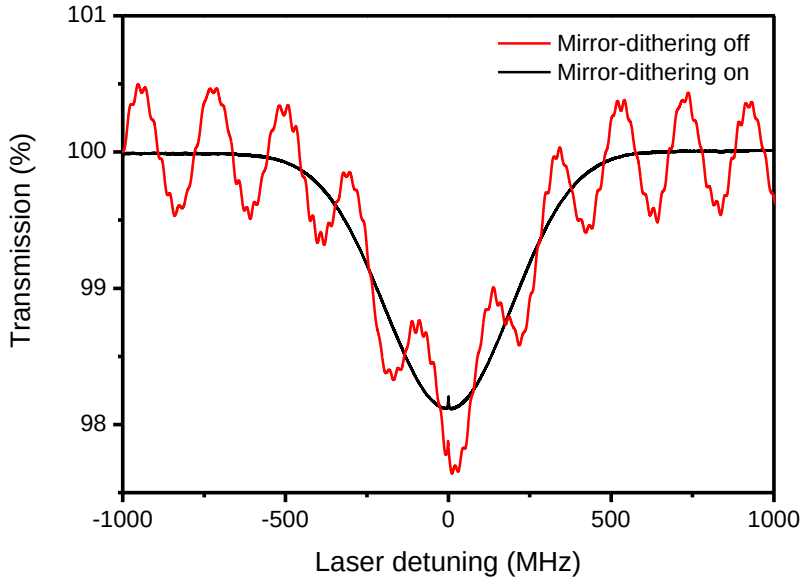

Figure 8. Unmodulated laser swept over a Doppler-broadened P(16) transition of $^{13}C_2H_2$ in a 2.8 Pa gas cell without and with the mirror dithering applied [Publication II].

Another factor strongly affecting the frequency of the laser's lock-point is the geometric arrangement of the pump and probe beams inside the gas-cell absorber. An angular mismatch between the wave fronts traveling to opposite directions inside the gas cell causes a frequency shift to the saturated absorption signal as the wave fronts interact with molecules belonging to a group that has a non-zero velocity component in the direction of the beams [Publication IV,85]. Unlike in our set-up, in the arrangements where resonators are employed to enhance the signal from the gas-cell absorber, the resonator fields inherently overlap. In our set-up, the collimation of the beams was ensured by carefully adjusting the position of the beam waist to the end mirror right behind the acetylene cell by maximizing the amount of light coupled back to the fiber. An aspheric lens with a relatively long focal length was employed to maximize the Rayleigh-range (,i.e., the distance from the waist of a Gaussian beam to the point where the beam cross-section area is doubled), and thus to minimize the wavefront curvature along the free-space beam traveling inside the acetylene cell.

Related to our fiber-based scheme an interesting approach to acetylene spectroscopy presented by Henningsen et al. in [86] is worth mentioning here. They have measured

saturated absorption of C_2H_2 molecules confined in the hollow core of a photonic bandgap fiber. However, SNR of the measurement needs to be improved to fully exploit this technique in realization of accurate wavelength standards.

Absolute frequency measurement results

It is possible to lock the acetylene-stabilized laser to over 25 lines in the ($\nu_1+\nu_3$) overtone band of $^{13}C_2H_2$ on covering a frequency band of wider than 2 THz. We measured the absolute frequency of the stabilized-laser locked to five different transitions of acetylene with a Ti:Sapphire optical frequency comb generator. For the measurements, the output of the acetylene-stabilized laser at 1.5 μm was frequency doubled using a periodically poled lithium niobate (PPLN) waveguide device to reach the wavelength range of the comb. The periodicity of the structure in the custom made PPLN waveguide device was chirped along the length of the crystal to enable frequency conversion over extended frequency band. The device provides about 1 mW of power at second harmonic when 250 mW of power within the wavelength range of 1530–1570 nm is taken to its input. Table II shows the results of the absolute frequency measurements compared to the values recommended by CIPM [6]. The values were consistent with CIPM values within the uncertainties of 3.6 kHz (k = 2).

Table II. Measured frequencies of the laser locked to five transitions of $^{13}C_2H_2$.

$^{13}C_2H_2$ transition	Frequency (kHz)	u_c (kHz)	Difference to the CIPM [6] value (kHz)
P(16)	194369569384.3	1.8	0.3
P(15)	194446632391.8	1.8	0.8
P(14)	194523020608.7	1.8	-1.3
P(11)	194748141655.4	1.8	-0.6
P(10)	194821826415.7	1.8	-0.3

The main uncertainty components arise from the repeatability of the measurements, the uncertainty of the modulation amplitude, and the uncertainty of the cell pressure. The

frequency shifts due possible changes in alignment have also been taken into account in the uncertainty estimate. The relative long-term stability (t = 1000 s) of the acetylene-stabilized laser is better than 10^{-12} and limited by white frequency noise. The measured Allan standard deviation [87] of the laser frequency is shown in Figure 9.

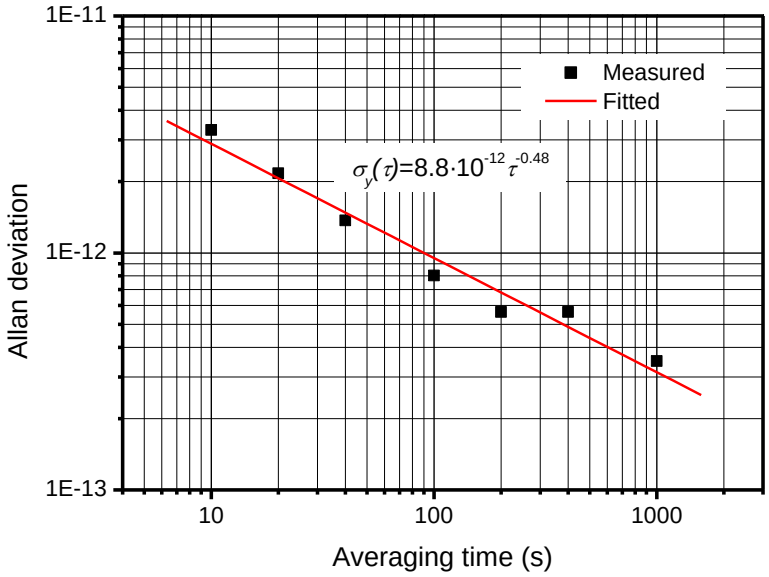

Figure 9. Typical Allan standard deviation of an acetylene P(16) line frequency measurement. [Publication II].

3.3.2 Optical single-frequency synthesizer

The single frequency synthesizer constructed in this work was designed for generating a single user-specified frequency from an atomic time base within the 192–196 THz gain bandwidth of an erbium-doped fiber amplifier (EDFA). The synthesizer is based on the ECDL, whose output is frequency doubled using a PPLN waveguide device and phase locked to a predetermined frequency component of a Ti:Sapphire optical frequency comb generator using an electrical PLL. By tuning the repetition rate of the Ti:Sapphire laser, the synthesized optical frequency can be swept with sub-kilohertz resolution. Frequency sweeps of several gigahertz are realized by automatically re-locking the ECDL to adjacent comb components during a frequency sweep. Figure 10 shows the principle of the frequency tuning. The re-locking method, demonstrated in this work,

allows sweeping the optical frequency, in principle, over the whole gain bandwidth of the EDFA.

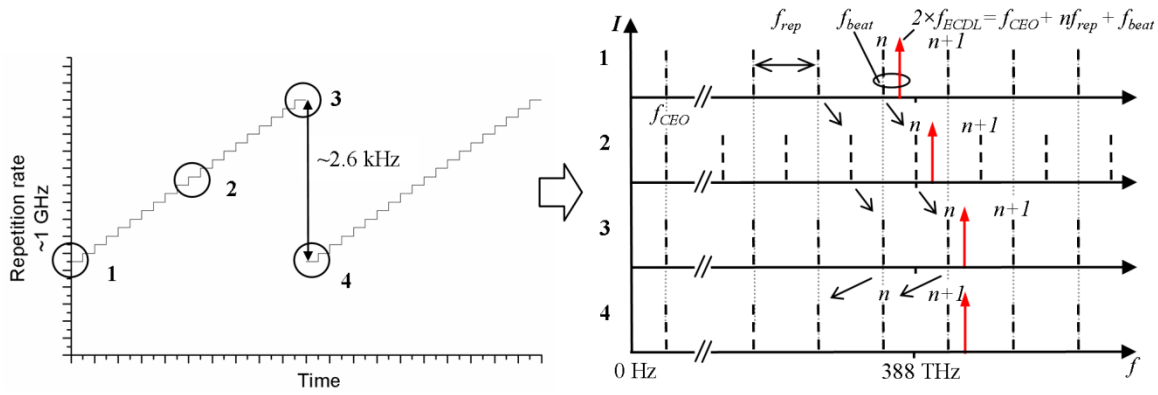

Figure 10. Tuning of the synthesized frequency. The left part of the figure illustrates the stepping of the repetition rate and the right part that of the optical frequencies. 1) The second harmonic of the synthesized frequency is locked to the n^{th} frequency component of the comb. 2-3) By stepping the repetition rate, the n^{th} component is shifted to the initial position of the $(n+1)^{th}$ component. 4) The repetition rate is set back to the start value and the synthesizer locks to the $(n+1)^{th}$ component [Publication III].

Line profile measurements of $^{13}C_2H_2$

We have utilized the synthesizer for direct Doppler-free spectroscopy on acetylene without modulation techniques [Publication III,IV]. High intensity stability of the synthesized signal and the capability of repeating the measurements on absolute frequency scale allowed performing line profile measurements at near infrared in unprecedented accuracy. The optical part of the set-up was essentially the same as that used in the acetylene-stabilized laser measurements. Indeed, we could alternate between these two configurations within minutes, just by rearranging electrical connections of the set-up. This offered an interesting possibility of investigating the effect of the different techniques of measurements of spectral lines.

Figure 11 shows a measurement over Doppler-broadened P(16) line on (ν_1+ ν_3) overtone band of acetylene. The measurement was done using 1-MHz step size. Due to frequency resolution the Lamb dip in the middle of the absorption curve is not shown properly. The inset in Figure 11 shows a measurement over the Lamb dip of the same transition in 79-kHz resolution. The intensity of the Lamb dip is less than 0.1 % of the

total detected power. The graph shown is an average of 31 similar measurements. The amplitude noise of the measurement is suppressed to practically negligible level by averaging.

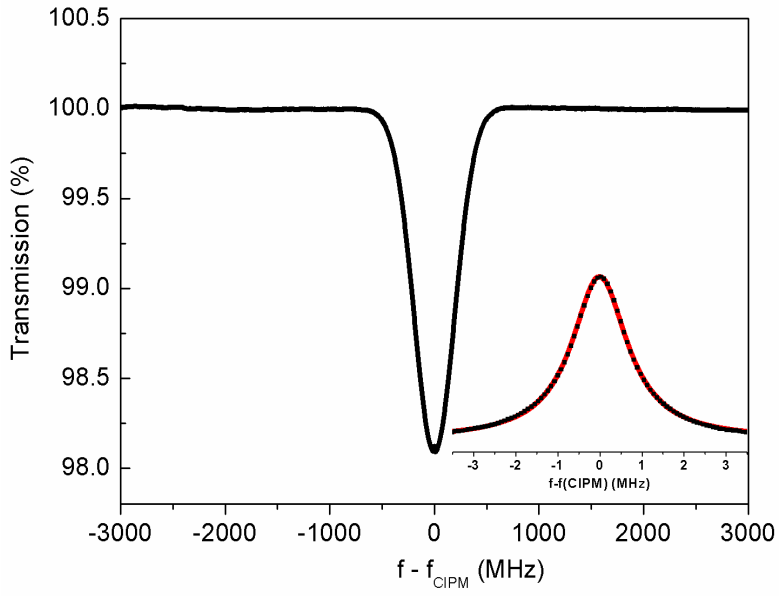

Figure 11. Doppler-broadened P(16) transition of acetylene at (v_1+v_3) overtone band recorded with the synthesizer. Inset: Doppler-free line shape of the same transition. The saturation dip spans a change of 0.08 % in transmission.

When the Gaussian profile of the Doppler-broadened line is subtracted, the true natural line shape of the transition can be investigated. By fitting a Lorentzian profile

$$I(f - f_0) = I_0 + \frac{2A}{\pi} \frac{w}{4(f - f_0)^2 + w^2} \qquad (11)$$

to the measurements, line shape asymmetry and the line center frequency could be determined. In equation (11) I_0 is the detected power offset, f_0 is the central frequency, w is full width at half-maximum, and A is the integrated area under Lorentzian profile. Figure 12 shows a Lorentzian and a Lorentzian with a dispersive term

$$I(f - f_0) = I_0 + [1 + B(f - f_0)] \frac{2A}{\pi} \frac{w}{4(f - f_0)^2 + w^2}, \qquad (12)$$

fitted to the measured line shape. In equation (12) *B* is a fit coefficient that sets the dispersive term strength. The residuals of the fits are shown in the lower part of Figure 12. The dispersive shape is addressed mainly due to a slight angular mismatch of the pump and probe beam, which might have remained despite of careful alignment.

Further, the residuals in Figure 12 indicate that in addition to dispersive shape, the signal is slightly too peaked. This might be a result of the increased relative contribution of slow molecules to the signal. When the linewidth is transit-time limited as in this measurement, the saturation becomes inhomogeneous for low pump laser powers and low gas pressures, and the line shape tends towards sharper peaking [88].

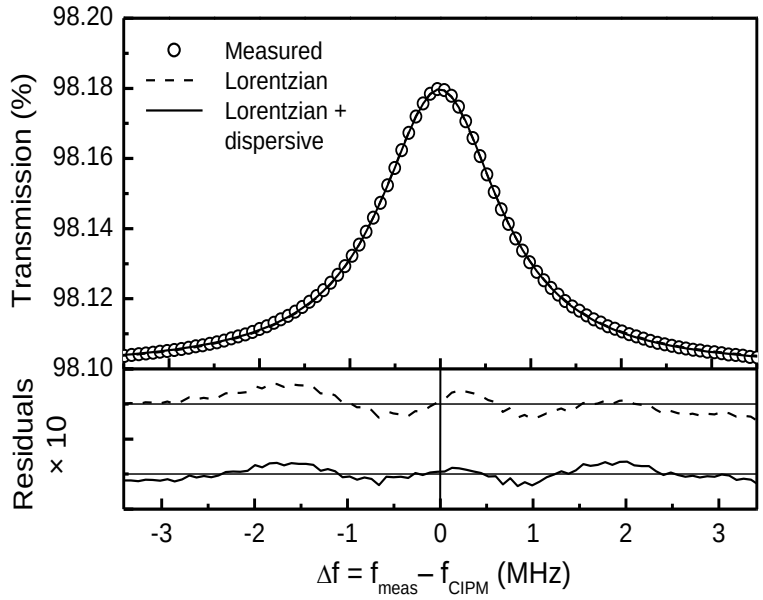

Figure 12. Measured P(16) line, a Lorentzian fit, Lorentzian + dispersive fit. Lower part shows residuals of the fits respectively [Publication IV].

We compared the line center values returned by the fits to the line center frequencies obtained using the acetylene-stabilized laser. To verify that the alignment had not changed between the two sets of measurement, we re-measured the absolute frequency of the P(16) line with the acetylene-stabilized laser right after the line shapes were measured with the synthesizer. The ability of rearranging the set-up between these two measurement modes enabled us to keep all the parameters related to optical set-up

constant. The re-measured absolute frequency of P(16) matched well with the value measured earlier with the stabilized-laser.

When the modulation shift in the acetylene-stabilized laser measurements is taken into account, the line center values obtained with the two methods agree within a few kilohertz, which is well within the combined uncertainty of 4.6 kHz (k = 2) of the measurements. The results gave also a very good match to the CIPM values. Table III sums the result. Regarding the acetylene-stabilized laser measurements the result of the P(16) line represents the re-measured value. The results shown for the lines P(10)–P(15) are taken from the earlier measurements with the stabilized-laser shown in Table II.

Table III. Measured frequencies of five $^{13}C_2H_2$ lines. Calculated modulation shifts are added to synthesizer frequencies.

line	synthesizer f_{synth} (kHz)	$^{13}C_2H_2$-stab.laser f_{stab} (kHz)	CIPM value (kHz)	$f_{synth} - f_{stab}$ (kHz)
P(10)	194821826415.9	194821826415.7	194821826416	0.2
P(11)	194748141655.5	194748141655.4	194748141656	0.1
P(14)	194523020606.4	194523020608.7	194523020610	–2.3
P(15)	194446632391.4	194446632391.8	194446632391	–0.4
P(16)	194369569382.1	194369569384.2	194369569384	–2.1

The effect of the modulation shift was studied also by numerical simulations using MATLAB/SimuLink software. We simulated the third-harmonic locking with lock-in amplifier servo loop and using the Lorentzian with a dispersive line shape component. The average modulation shift (-3.7±0.7) kHz/MHz returned by the simulations on four fitted P(16) line shapes was in good agreement with the experimentally measured modulation shift (-3.1±0.1) kHz/MHz of P(16) line [Publication II].

4 Indistinguishable single photons

A thorough understanding of the physical world requires that natural phenomena are examined not only on macroscopic level, where ensemble averages of particles and events are observed. When the examination is taken to individual particle level, the true quantum mechanical behavior of the events can be investigated.

Photons are often used in quantum mechanical experiments, as photon states are relatively easy to prepare and measure. One of the most fundamental group of experiments is the one where interference effects of single photons are investigated [89,90]. Interestingly, the results on a single-photon level differ drastically from that of the ensemble average. Although the motivation for the early experiments on the field was testing the theories of quantum mechanics [91,92], the recent progress has lead to potential applications in the field of optical quantum information processing. Such applications include optical quantum computing [93], communication, and cryptography [94]. Commercial applications in quantum cryptography already exist [95]. Communication with single photons by quantum teleportation has been demonstrated over long distances [96], and chip scale all-optical quantum computation has been demonstrated in laboratory conditions [97].

4.1 Single-photon sources

The key component for the applications mentioned above is a reliable single-photon source, which emits one and only one photon per defined time interval with high probability. The most straightforward solution would be to utilize a laser producing faint pulsed radiation. Laser output can be attenuated until the probability of finding more than one photon per pulse in a mode gets small. However, this method has a rather severe drawback. As the number of photons in coherent laser output is governed by Poisson statistics, most of the time the number of the photons in the mode would be zero. This limits the applicability of the laser source, as typically when a measurement should be made no photon would exist. Another approach using lasers utilizes a

spontaneous parametric down-conversion (SPDC) process, where correlated photon pairs are generated from higher frequency pump photons in a nonlinear crystal. Although the number of photons is statistically Poisson distributed also in this approach, the measurement of other photon (idler) can be used to inform that the other photon (signal) exists, thus reducing the number of measurements where no photons exist.

A two-level system can be operated as a natural single-photon source, as it inherently emits only one photon per one excitation-relaxation cycle. Single-photon action has been successfully demonstrated with molecules [98], atoms [99], ions [100], quantum dots [101], and diamond nitrogen-vacancy centers [102].

In recent years, active research has been undertaken to develop single-photon sources that are capable of emitting single-photons that are indistinguishable from each other. Motivation for this has been the requirement that quantum computation sets for a single-photon source: As quantum computation with linear optics relies on manipulation of entangled photon states [103], the emitted photons have to be indistinguishable. That is to say, they should be in the same optical mode, hence would share the same spectral and spatial features, and have the same optical polarization. Additionally, the emission process should be natural lifetime limited, i.e., no external influence on emission process should appear. Moreover, for practical applications, the sources should be scalable to multiple similar sources that exhibit mutual indistinguishability.

In the first experiments, trains of indistinguishable single photons were generated using single two-level emitters [104,105,106] as sources. Recently, indistinguishability of photons emitted from independent two-level emitters has been demonstrated in several experiments by quantum interference. This has been shown using independently trapped atomic emitters [107,108], quantum well nano-structures [109], and single molecules [23] as sources.

4.1.1 Characterization of single-photon sources

To validate the single-photon nature of a light source, one has to measure the second order intensity correlation [110]

$$g^{(2)}(\tau) = \frac{\langle I(t+\tau)I(t)\rangle}{\langle I(t)\rangle^2}, \qquad (13)$$

where *I(t)* is the average intensity with fixed time delay of τ for the consequently emitted photons, using a Hanbury Brown and Twiss (HBT) type of a set-up [111] shown in Figure 13.

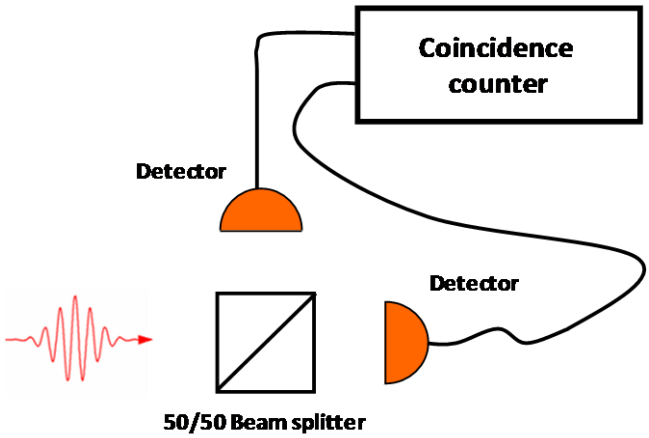

Figure 13. Hanbury Brown and Twiss type of photon correlation set-up.

The photons emitted by a source are sent to a 50/50 beam splitter. Single-photon detectors are placed at both outputs of the beam splitter. Time delays between clicks, i.e. photon arrivals, on the two detectors are recorded. Ideally, in the case of a true single-photon source, both detectors can not click simultaneously. Thus, the $g^{(2)}$-function is suppressed at τ = 0. Figure 14 shows a result of such a measurement recorded from a single-molecule light source using avalanche photon detectors (APD). The fact that the function in Figure 14 does not reach zero at τ = 0 implies that in addition to the signal from the single-molecule, some background signal is also present.

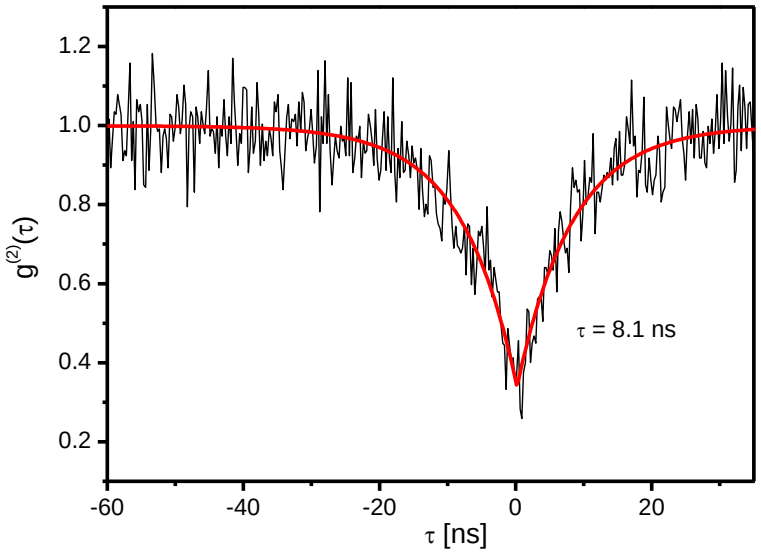

Figure 14. Second order photon correlation measurement of a single-photon source [Publication VI].

Photon indistinguishability is determined by a quantum interference measurement. Two photons are taken to a beam splitter from neighboring input ports. If the photons are in the same polarization state and their spectral and spatial modes perfectly overlap, the photons will coalesce and always leave the beam splitter together to the same direction (see Figure 15).

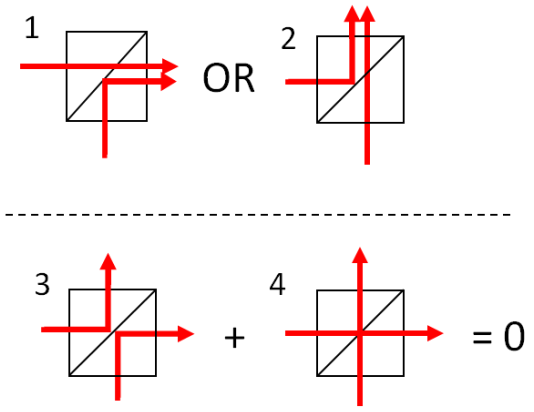

Figure 15. When identical single photons enter a 50/50 beam splitter from neighboring input ports they coalesce and leave the beam splitter always together (1 & 2). The probability amplitudes for the photon states where both photons are reflected or transmitted cancel each other (3 & 4) [92].

Essentially a similar HBT set-up, which was described above, can also be used for a quantum interference measurement. A correlation function is measured as a function of a delay between photon arrivals at a beam splitter. The experimental arrangement is illustrated in Figure 16. In case of an ideal spontaneous-emission single-photon source, a zero reaching dip in the function is observed when the delay between the two photons is tuned to zero as shown in Figure 17 by a theoretical correlation function [104]

$$g^{(2)}(\delta\tau) = 1 - \exp(-|\delta\tau| / \tau_s), \tag{14}$$

where $\delta\tau$ is the delay and τ_s corresponds to the spontaneous emission lifetime. The two-photon interference was experimentally first shown by Hong, Ou, and Mandel in 1987 [92] in an experiment where they used single photons from a SPDC source.

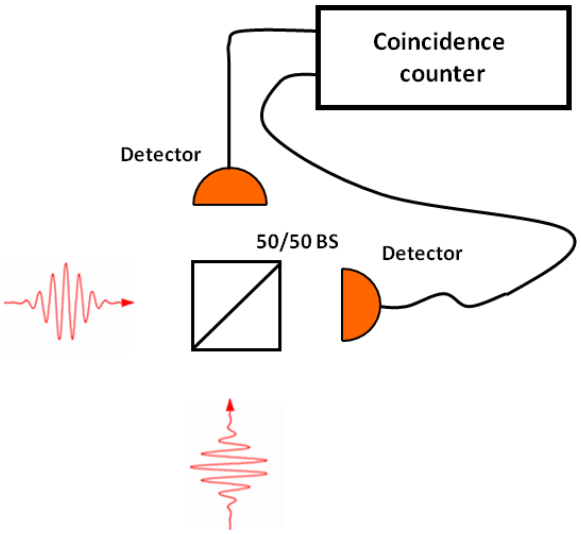

Figure 16. Hanbury Brown and Twiss type of set-up is used for measuring quantum interference between two indistinguishable photons.

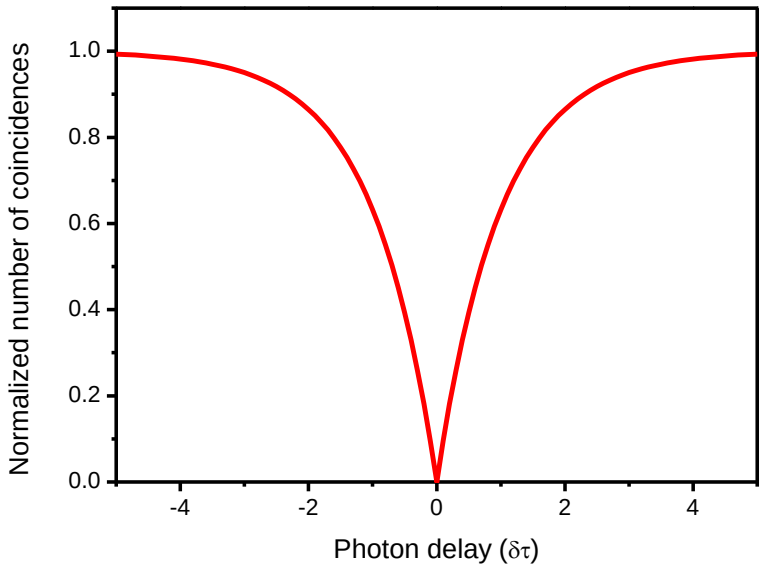

Figure 17. When the delay between indistinguishable single photons at a beam splitter is tuned to zero a deep dip in the measured correlation function occurs.

4.2 Low-temperature single molecules as single-photon sources

Single-molecule spectroscopy originates from 1989 when single molecules were detected for the first time by recording an absorption signal of an organic dye molecule embedded in a solid crystalline host at low temperature [112]. Soon after that, single-molecule detection based on fluorescence excitation spectroscopy was demonstrated [113]. Low temperature, single-molecule spectroscopy takes advantage on the effect of inhomogeneous broadening of molecular lines. A dilute solution of dye molecules in a crystalline host matrix is cooled to liquid helium temperatures (T < 4 K). At cryogenic temperatures the lines of the molecules get narrower as thermal effects are dramatically suppressed. Additionally, as the dye molecules are embedded in non-ideal crystalline host matrix, every molecule sees its environment a little differently, which leads to non-uniform shifting of the resonance frequencies of the molecules. Using a frequency tunable single-mode laser, one can individually select molecules by scanning the laser frequency over the inhomogeneously broadened absorption band of the molecules. In

detection, the excitation wavelength is filtered and fluorescence at longer wavelength is measured.

Organic molecules embedded in a crystalline host matrix offer an attractive system for studying quantum interference. At low temperatures, some electronic transitions become natural lifetime limited and offer quantum yield approaching unity. Further, the solid-state approach enables long observation times using the same emitters. In this work, the use of single molecules as sources of indistinguishable single photons was experimentally studied.

4.3 Experimental arrangement

The experimental work presented here has been carried out at the Laboratory of Physical Chemistry of Swiss Federal Institute of Technology Zurich (ETH). The objective of the research was to construct and characterize a set-up for demonstrating quantum interference using independent single molecules as single-photon sources. In Publication V we reported, for the first time, generation of indistinguishable single photons using two distinct single molecules. Organic fluorescent dibenzanthanthrene (DBATT) molecules in n-tetradecane were used as emitters and investigated by means of high resolution laser spectroscopy. DBATT molecules were chosen as candidate as previous studies have shown that DBATT embedded in crystalline host matrix at low temperatures has many properties that are desirable for a indistinguishable single-photon source, including near lifetime-limited linewidth, very weak triplet yield [114], and well defined orientation of the dipole moment [115].

High spatial resolution was obtained by preparing a molecule sample on a solid-immersion lens (SIL) through which the excitation laser radiation was focused using an aspheric lens. Photon correlation measurements on individual molecules under cw laser excitation proved the isolation of single quantum systems. Local electric fields were applied to match the emission wavelengths of the two molecules via DC-Stark effect.

In later state of the project, reported in Publication VI, a pulsed laser was included in the set-up and triggered generation of indistinguishable single photons was demonstrated.

To our knowledge, this was the first demonstration of single-molecule spectroscopy using pulsed excitation combined with high spectral and spatial resolution.

After the work described in this thesis, the set-up has been further developed and at the time of writing a quantum interference experiment using the set-up was reported [23]. The next sections sum up the experimental aspects essential for this work.

4.3.1 Excitation schemes

A dye molecule embedded in solid host matrix can be approximated as a two-level emitter. The energy levels of a dye molecule can be modeled with a simplified level scheme (Jablonsky diagram [116]) shown in Figure 18.

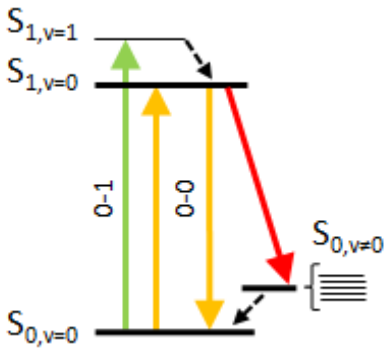

Figure 18. A simplified level scheme of a single dye molecule embedded in solid host matrix [Publication VI].

The relevant energy levels consist of the ground level and the first excited electronic level, denoted by $S_{0,v}$ and $S_{1,v}$ respectively. Both levels further contain a number of vibrational energy levels ($v \neq 0$). In this simplified level scheme, the probability for the molecule to enter to a metastable triplet state is considered negligible and has been ignored. It is possible that the molecule is excited also to a higher electronic state by multiple photon excitation. However, the lifetime of these states is very short (ps) and they decay non-radiatively to the first electronic level thus eliminating a possibility for two or more photon emission. In temperatures below 2 K, the purely electronic zero-phonon-line (ZPL) transition, i.e., the transition between the lowest levels of the ground

($S_{0,v=0}$) and the first excited electronic state ($S_{1,v=0}$) (denoted here as 0-0 ZPL), becomes natural lifetime limited. A DBATT molecule has a natural linewidth of about 17 MHz (FWHM) for a transition at a wavelength of λ = 590 nm.

There are two principal ways to excite the narrow linewidth molecules at cryogenic temperatures. The first method excites the molecule from the ground state $S_{0,v=0}$ into the $S_{1,v=0}$ state. From there the molecule decays back into the ground state and into a manifold of states with $v \neq 0$. The red shifted photons are detected, but the photons from the narrow 0-0 ZPL cannot be separated from the excitation laser light. This technique of photoluminescence excitation spectroscopy can directly measure the linewidth of the 0-0 ZPL by scanning a narrow band laser across the resonance.

In a second method, one excites the molecule into a higher vibrational level of the electronically excited state $S_{1,v=1}$. This state decays non-radiatively within a few ps into the state $S_{1,v=0}$, from which the molecule decays, giving access to photons emitted by the natural lifetime limited 0-0 ZPL. Transition from the ground state to $S_{1,v=1}$ is relatively broadband (about 30 GHz) due to short lifetime of $S_{1,v=1.}$

To identify lifetime limited single photons we spectrally scanned across the sample with a wavelength tunable cw dye laser and measured the 0-0 ZPL linewidths of potential molecules. After finding an isolated single molecule with a narrow 0-0 ZPL a second laser source was switched for pulsed 0-1 excitation. Thus, triggered 0-0 ZPL emission could be collected.

4.3.2 Spatial resolution

In addition to spectral resolution, high spatial resolution is needed. Spatial resolution is needed first of all to be able to locate an individual molecule and to reduce the background signal caused by weak excitation of nearby molecules. Thus, the spatial resolution should be sufficiently high so that no more than one molecule is resonant with the excitation laser in the focal volume at a time. High spatial resolution is especially important when higher vibrational states are excited with a pulsed laser. This

is due to the broad linewidth of the vibronically excited states. This together with the broad linewidth of the laser severely limits the possibility to spectrally select the molecules and hence puts greater emphasis on spatial resolution.

The spatial resolution is fundamentally limited by diffraction. The minimum obtainable FWHM spot size for a plane wave focused with a lens can be approximated as [117]

$$FWHM = \frac{\lambda}{2NA}, \tag{15}$$

where λ is the wavelength of the incident radiation and NA is the numerical aperture of the lens defined as

$$NA = n \cdot \sin(\theta_{½}), \tag{16}$$

where n is the refractive index of the medium where the lens operates and $\theta_{½}$ is the half angle subtended by the lens. We achieved a tight focus by employing an aspheric lens with a NA of 0.55 (in air) together with a solid immersion lens (SIL) made from cubic zirconia (ZrO_2), whose refractive index is 2.2. The sample is prepared in between the flat side of the SIL and a glass substrate. The incident light is focused into the sample through the SIL. Because the light is focused to the center of the hemispherical lens no refraction at the outer edge of the lens occurs. Hence SIL gives direct improvement of the focused spot size by factor of n. It should be noted that in a case where the laser beam is focused through the lens the dimension limiting the spot size is usually the beam diameter. However, equation (15) gives the theoretical upper limit for the resolution of the lens system.

The emitted photons are collected using the same lens system. The high refractive index of the SIL also improves the light collection efficiency, which is crucial in the single-photon applications. Figure 19 shows a schematic view of the arrangement.

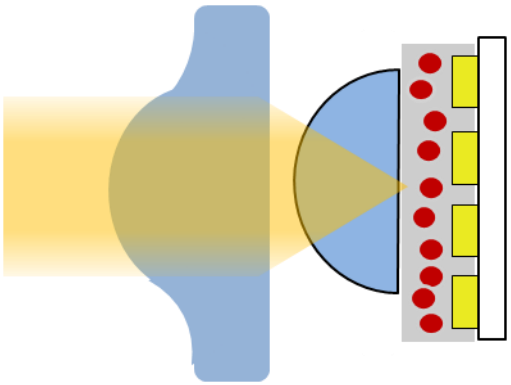

Figure 19. Laser light is focused into the molecule sample using aspheric and solid immersion lenses. The sample has been prepared on gold electrodes to enable Stark shifting the lines.

4.3.3 Stark shifting the lines of the molecules

We exploited the DC-Stark effect to shift the transition frequencies of two molecules in distinct samples to match each other. This was done by applying a static electric field over the molecules on one of the samples. The electric field was applied using gold electrodes under the samples (see Figure 19). The narrow spacing of interdigitated electrodes, 18 µm, makes it possible to reach high electric fields on the order of 10^6 V/m with voltages below 100V. With this configuration we typically found shifts in the zero-phonon-lines of the molecules in the order of ~100 Hz/(V/m). Figure 20 shows an example where nearly natural lifetime limited zero-phonon-lines of two independent DBATT molecules in distinct samples are detected simultaneously. The molecule whose line is initially at higher frequency is frequency shifted across the line of the other molecule, thus making the 0-0 zero-phonon-lines of the molecules spectrally indistinguishable at the point where the lines cross.

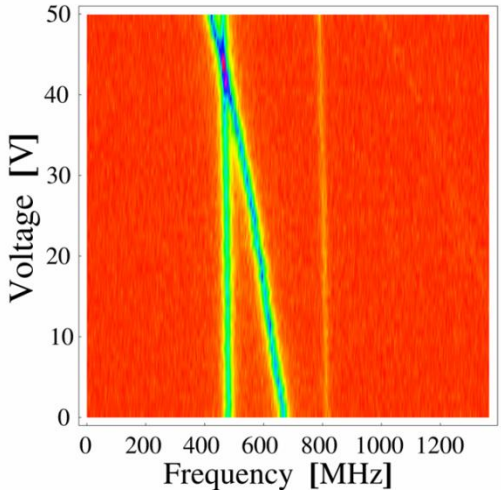

Figure 20. Fluorescence excitation spectra of two molecules in distinct samples. The vertical axis shows the voltage applied on electrodes and horizontal axis the frequency sweep of the laser. An electric field applied to one of the molecules shifts its line to lower frequencies with increasing voltage. [Publication VI].

4.3.4 Continuation of the project

Experimental aspects presented above demonstrated the capability of using independent single molecules to generate indistinguishable single photons. As explained before, true quantum indistinguishability requires identical photons with respect to wavelength, polarization state, and spatial mode. DBATT molecules embedded in a crystalline host matrix have well-oriented transition dipole moments whose emission can be linearly polarized. Thus, the polarization of the emitted photons can readily be matched. Furthermore, the emission from single molecules can be coupled into to a single-mode fiber with an efficiency of 30 % or more, which conveniently ensure spatial mode matching. Indeed, after the work done for this thesis, two-photon interference was demonstrated using the set-up [23]. Single-photon beams from two molecules were coupled into the two arms of a single-mode polarization maintaining fiber beam splitter. Half-wave plates were used to align the input polarizations. A photon correlation measurement at the output arms of the fiber-optic beam splitter showed a clear sign of quantum interference.

The high photostability and the compact solid-state arrangement of the sources allow nearly indefinite measurement times on the same emitter and a straightforward up-

scaling to a larger number of identical single-photon sources. These results are promising for miniaturization and integration of several single-photon sources to ever smaller volumes, even on a single chip.

5 Conclusions

In this work, advanced applications based on the utilization of wavelength tunable lasers in optical radiometry, optical frequency metrology, and quantum optics were studied and developed.

In the field of optical radiometry, a study of different techniques for measuring absolute spectral irradiance responsivity was carried out. A comparative study of spectral irradiance responsivity measurement techniques was performed between measurement systems used for detector calibrations at TKK and NIST. Two laser-based and a monochromator based measurement systems were compared by measuring the absolute spectral irradiance responsivity of a near infrared filter radiometer with each system. The work provided the first reported results of a detailed comparison of different calibration techniques for spectral irradiance responsivity at near infrared wavelength region. The study showed excellent agreement between the three calibration systems and gave validation for the low uncertainty, below the level of 0.1 %, stated for both laser-based calibration systems. The results have significant implications for radiation thermometry and a number of other radiometric applications where high accuracy spectral radiance and irradiance measurements are crucial.

In a work done at MIKES, an acetylene-stabilized laser and an optical single-frequency synthesizer were constructed and characterized. The acetylene-stabilized laser was realized, for the first time, by taking a fiber-based approach. By dithering the length of the optical path in the spectroscopy arrangement, interference inherently present in a fiber-based scheme was effectively suppressed by averaging. Conceivably, the mirror dithering technique could be generally applied to frequency-stabilized lasers based on external gas cells to improve long term stability through the reduction of slowly varying frequency-dependent intensity changes caused by interference. Absolute frequency measurements of the laser stabilized to five different lines of acetylene were in good agreement with the values recommended by CIPM with a standard uncertainty of 1.8 kHz. The relatively straightforward construction of the acetylene-stabilized laser

provides a potential for developing compact and portable wavelength standards in telecommunication wavelengths.

The optical single-frequency synthesizer was designed for generating a user-specified frequency from an atomic time base within the 192–196 THz gain bandwidth of an EDFA. A phase-coherent link between microwave and optical frequencies was established using an optical frequency comb generator. Scanning the optical frequency was realized by stepping the repetition rate of the optical frequency comb generator. Combined with a comb component handover process, this method allows, in principle, scanning the optical frequency over the entire gain bandwidth of the EDFA with sub-kilohertz resolution. The capability of repeating the measurements on absolute frequency scale and the high intensity stability of the synthesizer enabled performing spectroscopy without modulation techniques in unprecedented accuracy at telecommunication wavelengths. In addition to spectroscopy, the developed synthesizer is directly suitable for characterization of optical components used in telecommunication networks.

The synthesizer was utilized for recording the shapes of acetylene transitions and studying their lineshape asymmetries by theoretical fits. The high signal-to-noise ratio of the measurement enabled determination of absolute line-center frequencies with 1.4 kHz uncertainty. The line-center frequencies were in excellent agreement with the frequencies obtained with the acetylene-stabilized laser and with the CIPM values. The calculated modulation shift based on the fitted asymmetrical line shape agreed with the shift determined from acetylene-stabilized laser measurements. Thus, origin of the modulation shift in the third-harmonic measurement could be determined.

The final part of the work presented in this thesis was carried out at ETH in Zurich. A light source emitting indistinguishable single photons from independent single molecules was developed. For the first time, a solid-state source consisting of multiple independent emitters was used to emit indistinguishable single photons.

By means of high resolution laser spectroscopy and optical microscopy in cryogenic conditions, two fluorescent molecules under distinct microscopes were detected. Fluorescence excitation spectroscopy with a wavelength tunable cw dye laser was

utilized to detect and measure natural lifetime limited zero-phonon-lines of the molecules in two distinct samples. Vibronic excitation with a pulsed laser allowed collecting triggered zero-phonon-line emission. The utilization of solid immersion lenses together with aspheric lenses enabled high spatial resolution. By exploiting DC-Stark shifts, the resonances of the detected molecules were shifted to match each other. Later measurements verified the indistinguishability of the photons by quantum interference measurements. The work has implications on the development of various quantum information processing schemes.

The techniques explored in the thesis show the extraordinary power and application that wavelength tunable lasers can provide in exploring limits of measurement science and fundamental studies in physics.

References

[1] A. L. Schawlow and C. H. Townes, "Infrared and optical masers," Phys. Rev. **112**, 1940–1949 (1958).

[2] T. H. Maiman, "Stimulated optical radiation in ruby," Nature **187**, 493–494 (1960).

[3] W. Demtröder, "Laser Spectroscopy," Vol. 1, 4th ed., Springer 2008, 457 p., ISBN 978-3-540-73415-4.

[4] A. Zeilinger, G. Weihs, T. Jennewein, and M. Aspelmeyer, "Happy centenary, photon," Nature **433**, 230–238 (2005).

[5] The International System of Units (SI), 8th Edition Bureau International des Poids et Mesures, Sèvres, France, 88 p. (2006).

[6] R. Felder, "Practical realization of the definition of the metre, including recommended radiations of other optical frequency standards," Metrologia **42**, 323–325 (2005).

[7] H. S. Margolis, G. P. Barwood, G. Huang, H. A. Klein, S. N. Lea, K. Szymaniec, and P. Gill, "Hertz-Level Measurement of the Optical Clock Frequency in a Single $^{88}Sr^{+}$ Ion," Science **306**, 1355–1358 (2004).

[8] P. Dubé, A. A. Madej, J. E. Bernard, and L. Marmet, "A narrow linewidth and frequency-stable probe laser source for the $^{88}Sr^{+}$ single ion optical frequency standard," Appl. Phys. B **95**, 43–54 (2009).

[9] C. W. Chou, D. B. Hume, J. C. J. Koelemeij, D. J. Wineland, and T. Rosenband, "Frequency Comparison of Two High-Accuracy Al^{+} Optical Clocks," Phys. Rev. Lett. **104**, 070802 (2010).

[10] A. D. Ludlow, T. Zelevinsky, G. K. Campbell, S. Blatt, M. M. Boyd, M. H. G. de Miranda, M. J. Martin, J. W. Thomsen, S. M. Foreman, Jun Ye, T. M. Fortier, J. E. Stalnaker, S. A. Diddams, Y. Le Coq, Z. W. Barber, N. Poli, N. D. Lemke, K. M. Beck, and C. W. Oates, "Sr lattice clock at 1×10^{-16} fractional uncertainty by remote optical evaluation with a Ca clock," Science **319**, 1805–1808 (2008).

[11] "Principles governing photometry," Metrologia **19**, 97–101 (1983).

[12] ITU-T standard G.671, Transmission characteristics of optical components and subsystems.

[13] "Laser Marketplace 2009," Laser Focus World, January 2009.

[14] A. Javan, W. R. Bennet Jr., and D. R. Herriot, "Population inversion and continuous optical maser oscillation in a gas discharge containing a He-Ne mixture," Phys. Rev. Lett. **3**, 106–110 (1961).

[15] R. N. Hall, G. E. Fenner, J. D. Kingsley, T. J. Soltys, and R. O. Carlson, "Coherent light emission from GaAs junctions," Phys. Rev. Lett. **9**, 366–368 (1962).

[16] O. G. Peterson, S. A. Tuccio, and B. B. Snavely, "cw operation of an organic dye solution laser," Appl. Phys. Lett. **6**, 245–247 (1970).

[17] M. J. Weber, "Handbook of laser wavelengths," CRC Press LLC 1999, 767 p., ISBN 0-8493-3508-6.

[18] J. M. Yarborough, "cw dye laser emission spanning the visible spectrum," Appl. Phys. Lett. **24**, 629–630 (1974).

[19] P. F. Moulton, "Spectroscopic and laser characterization of Ti:Al_2O_3," J. Opt. Soc. Am. B **3**, 125–132 (1986).

[20] M. Fleming and A. Mooradian, "Spectral characteristics of external-cavity controlled semiconductor lasers", IEEE J. Quantum Electron **17**, 44–59 (1981).

[21] M. Noorma, P. Toivanen, F. Manoocheri, and E. Ikonen, "Characterization of filter radiometers with a wavelength-tunable laser source," Metrologia **40,** S220–S223 (2003).

[22] S. W. Brown, G. P. Eppeldauer, and K. R. Lykke, "Facility for spectral irradiance and radiance responsivity calibrations using uniform sources," Appl. Opt. **45,** 8218–8237 (2006).

[23] R. Lettow, Y. L. A. Rezus, A. Renn, G. Zumhofen, E. Ikonen, S. Götzinger, V. Sandoghdar, "Quantum interference of tunably indistinguishable photons from remote organic molecules," Phys. Rev. Lett. **104**, 123605 (2010).

[24] A. C. Parr, R. U. Datla, and J. L. Gardner, "Optical radiometry," Elsevier Inc. 2005, ISBN 0-12-475988-2.

[25] N. P. Fox, J. E. Martin, and D. H. Nettleton, "Absolute spectral radiometric determination of the thermodynamic temperatures of the melting/freezing points of Gold, Silver and Aluminium," Metrologia **28**, 357–374 (1991).

[26] P. Sperfeld, K.-H. Raatz, B. Nawo, W. Möller, and J. Metzdorf, "Spectral-irradiance scale based on radiometric black-body temperature measurements," Metrologia **32**, 43–439 (1996).

[27] H. W. Yoon, P. Sperfeld, S. Galal Yousef, and J. Metzdorf, " NIST-PTB measurements of the radiometric temperatures of a high-temperature black body using filter radiometers," Metrologia **37**, 377–380 (2000).

[28] M. Ojanen, V. Ahtee, M. Noorma, T. Weckström, P. Kärhä, and E. Ikonen, "Filter radiometers as a tool for quality assurance of temperature measurements with linear pyrometers," Int. J. Thermophysics **29**, 1084–1093 (2008).

[29] H. W. Yoon, C. E. Gibson, and P. Y. Barnes, "Realization of National Institute of Standards and Technology detector-based spectral irradiance scale," Appl. Opt. **41**, 5879–5890 (2002).

[30] H. Preston-Thomas, "The International Temperature Scale of 1990 (ITS-90)," Metrologia **27**, 3–10 (1990).

[31] R. E. Edsinger and J. F. Schooley, "Differences between Thermodynamic Temperature in the Range 230°C to 660°C and t (IPTS-68)," Metrologia **26**, 95–106 (1989).

[32] H. W. Yoon, D. W. Allen, C. E. Gibson, M. Litorja, R. D. Saunders, S. W. Brown, G. P. Eppeldauer, and K. R. Lykke, "Thermodynamic-temperature determinations of the Ag and Au freezing temperatures using a detector-based radiation thermometer," Appl. Opt. **46**, 2870–2880 (2007).

[33] J. E. Martin, N. P. Fox, and P. J. Key, "A Cryogenic Radiometer for Absolute Radiometric Measurements," Metrologia **21**, 147–155 (1985).

[34] J. M. Houston, and J. P. Rice, "NIST reference cryogenic radiometer designed for versatile performance," Metrologia **43**, S31–S35 (2006).

[35] T. C. Larason, S. S. Bruce, and A. C. Parr, "Spectroradiometric Detector Measurements: Part I–Ultraviolet Detectors and Part II–Visible to Near-Infrared Detectors, Natl. Inst. Stand. Technol. Spec. Publ. 250–41, U.S. Govt. Printing Office (1998).

[36] P. Kärhä, A. Haapalinna, P. Toivanen, F. Manoocheri, and E. Ikonen, "Filter radiometry based on direct utilization of trap detectors," Metrologia **35**, 255–259 (1998).

[37] V. E. Anderson, N. P. Fox, and D. H. Nettleton, "Highly stable, monochromatic and tunable optical radiation source and its application to high accuracy spectrophotometry," Appl. Opt. **31,** 536–545 (1992).

[38] S. W. Brown and K. R. Lykke, NIST, Gaithersburg, Md., personal communication, 2007.

[39] J. T. Woodwar, A. W. Smith, C. A. Jenkins, C. Lin, S. W. Browm, and K. R. Lykke, "Supercontinuum sources for metrology," Metrologia **46**, S277–S282 (2009).

[40] H. W. Yoon, P. Sperfeld, S. Galal Yousef, and J. Metzdorf, "NIST-PTB measurements of the radiometric temperatures of a high-temperature black body using filter radiometers," Metrologia **37**, 377–380 (2000).

[41] P. Kärhä, N. J. Harrison, S. Nevas, W. S. Hartree, and I. Abu-Kassem, "Intercomparison of characterization techniques of filter radiometers in the ultraviolet region," Metrologia **40**, S50–S54 (2003).

[42] N. P. Fox, “Trap detectors and their properties,” Metrologia **28,** 197–202 (1991).

[43] P. Toivanen, F. Manoocheri, P. Kärhä, E. Ikonen, and A. Lassila, “Method for characterization of filter radiometers,” Appl. Opt. **38**, 1709–1713 (1999).

[44] Documents Concerning the New Definition of the Metre, Metrologia **19**, 163–177 (1984).

[45] K. M. Evenson, J. S. Wells, F. R. Petersen, B. L. Danielson, and G. W. Day, “Accurate frequencies of molecular transitions used in laser stabilization: the 3.39-μm transitions in CH_4 and 9.33- and 10.18-μm transitions in CO_2,” Appl. Phys. Lett. **22**, 192–195 (1973).

[46] D. A. Jennings, C. R. Pollock, F. R. Peterson, R. E. Drullinger, K. M. Evenson, J. S. Wells, J. L. Hall, and H. P. Layer, “Direct frequency measurement of the I_2-stabilized He-Ne 473-THz (633 nm) laser,” Opt. Lett. **8**, 136–138 (1983).

[47] O. Acef, J. J. Zondy, M. Abed, D. G. Rovera, A. H. Gérard, A. Clairon, Ph. Laurent, Y. Millerioux, and P. Juncar, “A CO_2 to visible optical frequency synthesis chain: accurate measurement of the 473 THz HeNe/I_2 laser ,” Opt. Commun. **97**, 29–34 (1993).

[48] J. E. Bernard, A. A. Madej, L. Marmet, B. G. Whitford, K. J. Siemsen, and S. Cundy, “Cs-Based Frequency Measurement of a Single, Trapped Ion Transition in the Visible Region of the Spectrum,” Phys. Rev. Lett. **82**, 3228–3231 (1999).

[49] H. Schnatz, B. Lipphardt, J. Helmcke, F. Riehle, and G. Zinner, “First Phase-Coherent Frequency Measurement of Visible Radiation,” Phys. Rev. Lett. **76**, 18–21 (1996).

[50] T. G. Blaney, C. C. Bradley, G. J. Edwards, B. W. Jolliffe, D. J. E. Knight, and P. T. Woods, “Measurement of the frequency of the methane-stabilised laser at 3.39 μm and of the R(32) transition of CO_2 at 10.17 μm,” Nature **254**, 584–585 (1975).

[51] H. R. Telle, D. Meschede, and T. W. Hänsch, “Realization of a new concept for visible frequency division: phase locking of harmonic and sum frequencies,” Opt. Lett. **15**, 532–534 (1990).

[52] J. Reichert, R. Holzwarth, Th. Udem, T. W. Hänsch, “Measuring the frequency of light with mode-locked lasers,” Opt. Commun. **172**, 59–68 (1999).

[53] D. J. Jones, S. A. Diddams, J. K. Ranka, A. Stentz, R. S. Windeler, J. L. Hall, and S. T. Cundiff, “Carrier-envelope phase control of femtosecond mode-locked lasers and direct optical frequency synthesis,” Science **288**, 635–639 (2000).

[54] S. A. Diddams, D. J. Jones, J. Ye, S. T. Cundiff, J. L. Hall , J. K. Ranka, R. S. Windeler, R. Holzwarth, Th. Udem, and T. W. Hänsch, “Direct link between microwave and optical frequencies with a 300 THz femtosecond laser comb,” Phys. Rev. Lett. **29**, 5102–5105 (2000).

[55] R. Holzwarth, Th. Udem, T. W. Hänsch, J. C. Knight, W. J. Wadsworth, and P. St. J. Russell, "Optical Frequency Synthesizer for Precision Spectroscopy," Phys. Rev. Lett. **85**, 2264–2267 (2000).

[56] J. K. Ranka, R. S. Windeler, and A. J. Stentz, "Visible continuum generation in air-silica microstructure optical fibers with anomalous dispersion at 800 nm," Opt. Lett. **25**, 25–27 (2000).

[57] B. R. Washburn, S. A. Diddams, N. R. Newbury, J. W. Nicholson, M. F. Yan, and C. G. Jørgensen, "Phase-locked, erbium-fiber-laser-based frequency comb in the near infrared," Opt. Lett. **29**, 250–252 (2004).

[58] T. R. Schibli, K. Minoshima, F.-L. Hong, H. Inaba, A. Onae, H. Matsumoto, I. Hartl, and M. E. Fermann, "Frequency metrology with a turnkey all-fiber system," Opt. Lett. **29**, 2467–2469 (2004).

[59] Th. Udem, R. Holzwarth, and T. W. Hänsch, "Optical frequency metrology," Nature **416**, 233–237 (2002).

[60] G. Genty, M. Lehtonen, H. Ludvigsen, J. Broeng ,and M. Kaivola, "Spectral broadening of femtosecond pulses into continuum radiation in microstructured fibers," Opt. Express **10**, 1083–1098 (2002).

[61] R. Ell, U. Morgner, F. X. Kärtner, J. G. Fujimoto, E. P. Ippen, V. Scheuer, G. Angelow, T. Tschudi, M. J. Lederer, A. Boiko, and B. Luther-Davies, "Generation of 5-fs pulses and octave-spanning spectra directly from a Ti:sapphire laser," Opt. Lett. **15**, 373–375 (2001).

[62] H. M. Goldenberg, D. Kleppner, and N. F. Ramsay, "Atomic Hydrogen maser," Phys. Rev. Lett. **5**, 361–362 (1960).

[63] J. L. Hall, "Stabilized lasers and precision measurements," Science **202**, 147–156 (1978).

[64] T. W. Hänsch, I. S. Shanin, and A. L. Schawlow, "High-resolution saturation spectroscopy of the sodium D lines with a pulsed tunable dye laser," Phys. Rev. Lett. **27**, 707–710 (1971).

[65] A. J. Wallard, "Frequency stabilization of the helium-neon laser by saturated absorption in iodine vapour," J. Phys. E: Sci. Instrum. **5**, 926–930 (1972).

[66] G. R. Hanes, K. M. Baird, and J. DeRemigis, "Stability, reproducibility, and absolute wavelength of a 633 nm He-Ne laser stabilized to an iodine hyperfine component," Appl. Opt. **12**, 1600–1605 (1973).

[67] S. Picard, L. Robertsson, L-S Ma, K. Nyholm, M. Merimaa, T. Ahola, P. Balling, P. Kren, and J.-P. Wallerand, "Comparison of $^{127}I_2$-stabilized frequency-doubled Nd:YAG lasers at Bureau International des Poids et Mesures," Appl. Opt. **42**, 1019–1028 (2003).

[68] H.S. Margolis, "Frequency metrology and clocks," J. Phys. B: At. Mol. Opt. Phys. **42**, 154017 (2009).

[69] M. Merimaa, K. Nyholm, M. Vainio, and A. Lassila, "Traceability of laser frequency calibration at MIKES," IEEE Trans. Instrum. Meas. **56**, 500–504 (2007).

[70] J. Lazar, J. Hrabina, P. Jedlicka, and O. Cíp, "Absolute frequency shifts of iodine cells for laser stabilization," Metrologia **46**, 450–456 (2009).

[71] A. Czajkowski, A.A. Madej, and P. Dubé, "Development and study of a 1.5 μm optical frequency standard referenced to the P(16) saturated absorption line in the ($\nu_1+\nu_3$) overtone band of $^{13}C_2H_2$," Opt. Commun. **234**, 259–268 (2004).

[72] C. S. Edwards, H. S. Margolis, G. P. Barwood, S. N. Lea, P. Gill, G. Huang, W. R. C. Rowley, "Absolute frequency measurement of a 1.5-μm acetylene standard by use of a combined frequency chain and femtosecond comb," Opt. Lett. **6**, 566–568 (2004).

[73] P. Balling, M. Fischer, P. Kubina, and R. Holzwarth, "Absolute frequency measurement of wavelength standard at 1542 nm: acetylene stabilized DFB laser," Opt. Express **13**, 9196–2001 (2005).

[74] W. E. Lamb, "Theory of an optical maser," Phys. Rev. **134**, A1429–A1450 (1964).

[75] V. Gerginov, C. E. Tanner, S. A. Diddams, A. Bartels, and L. Hollberg, " High-resolution spectroscopy with a femtosecond laser frequency comb," Opt. Lett. **30**, 1734–1739 (2005).

[76] M. J. Thorpe and J. Ye, "Cavity-enhanced direct frequency comb spectroscopy," Appl. Phys. B **91**, 397–414 (2008).

[77] J. D. Jost, J. L. Hall, and J. Ye, "Continuously tunable, precise, single frequency optical signal generator," Opt. Express **10**, 515–520 (2002).

[78] H. Inaba, T. Ikegami, F.-L. Hong, Y. Bitou, A. Onae, T. R. Schibli, K. Minoshima, and H. Matsumoto, "Doppler-free spectroscopy using a continuous-wave optical frequency synthesizer," Appl. Opt. **45**, 4910–4915 (2006).

[79] S. E. Park, E. B. Kim, Y.-H. Park, D. S. Yee, T. Y. Kwon, C. Y. Park, H. S. Moon, and T. H. Yoon, "Sweep optical frequency synthesizer with a distributed-Bragg-reflector laser injection locked by a single component of an optical frequency comb," Opt. Lett. **31**, 3594–3596 (2006).

[80] A. K. Mills, Y.-F. Chen, K. W. Madison, and D. J. Jones, "Widely tunable, single-mode optical frequency synthesizer with a 100 kHz uncertainty," J. Opt. Soc. Am. B. **26**, 1276–1280 (2009).

[81] T. M. Fortier, Y. Le Coq, J. E. Stalnaker, D. Ortega, S. A. Diddams, C. W. Oates, and L. Hollberg, "Kilohertz-resolution spectroscopy of cold atoms with an optical frequency comb," Phys. Rev. Lett. **97**, 163905 (2006).

[82] H. Inaba, T. Ikegami, F.-L. Hong, Y. Bitou, A. Onae, T. R. Schibli, K. Minoshima, and H. Matsumoto, "Doppler-free spectroscopy using a continuous-wave optical frequency synthesizer," Appl. Opt. **45**, 4910–4915 (2006).

[83] B. R. Washburn, R. W. Fox, N. R. Newbury, J. W. Nicholson, K. Feder, P. S. Westbrook, and C. G. Jørgensen, "Fiber-laser-based frequency comb with a tunable repetition rate," Opt. Express **12**, 4999–5004 (2004).

[84] J. A. Silver and A. C. Stanton, "Optical interference fringe reduction in laser absorption experiments," Appl. Opt. **27**, 1914–1916 (1988).

[85] S. E. Park, H. S. Lee, T. Y. Kwon, and H. Cho, "Dispersion-like signals in velocity-selective saturated-absorption spectroscopy," Opt. Commun. **192**, 49–55 (2001).

[86] J. Henningsen, J. Hald, and J. C. Peterson, "Saturated absorption in acetylene and hydrogen cyanide in hollow-core photonic bandgap fibers," Opt. Express **13**, 10475-10482 (2005).

[87] D. W. Allan, "Statistics of Atomic Frequency Standards," P. IEEE **54**, 221–230 (1966).

[88] C. J. Bordé, J. L. Hall, C. V. Kunasz, and D. G. Hummer, "Saturated absorption line shape: Calculation of the transit-time broadening by a perturbation approach," Phys. Rev. A **14**, 236–263 (1976).

[89] L. Mandel, "Photon interference and correlation effects produced by independent quantum sources," Phys. Rev. A **28**, 929–943 (1983).

[90] H. Paul, "Interference between independent photons," Rev. Mod. Phys. **58**, 209–231 (1986).

[91] R. Ghosh and L. Mandel, "Observation of nonclassical effects in the interference of two photons," Phys. Rev. Lett. **59**, 1903–1905 (1987).

[92] C. K. Hong, Z. Y. Ou, and L. Mandel, "Measurement of subpicosecond time intervals between two photons by interference," Phys. Rev. Lett. **59**, 2044–2046 (1987).

[93] P. Kok, W. J. Munro, K. Nemoto, T. C. Ralph, J. P. Dowling, and G. J. Milburn, "Linear optical quantum computing with photonic qubits," Rev. Mod. Phys. **79**, 135–174 (2007).

[94] N Gisin, G. Ribordy, W. Tittel, and H. Zbinden, "Quantum cryptography," Rev. Mod. Phys. **74**, 145–195 (2002).

[95] Id Quantique SA, http://www.idquantique.com/, 10.5.2010.

[96] R. Ursin, T. Jennewein, M. Aspelmeyer, R. Kaltenbaek, M. Lindenthal, P. Walther, and A. Zeilinger, "Quantum teleportation across the Danube," Nature **430**, 849 (2004).

[97] A. Politi, J. C. F. Matthews, and J. L. O'Brien, "Shor's quantum factoring algorithm on a photonic chip," Science **325**, 1221 (2009).

[98] Ch. Brunel, B. Lounis, Ph. Tamarat, and M. Orrit, "Triggered Source of Single Photons based on Controlled Single Molecule Fluorescence," Phys. Rev. Lett. **83**, 2722–2726 (1999).

[99] A. Kuhn, M. Hennrich, and G. Rempe, "Deterministic Single-Photon Source for Distributed Quantum Networking," Phys. Rev. Lett. **89**, 067901 (2002).

[100] M. Keller, B. Lange, K. Hayasaka, W. Lange, and H. Walther, "Continuous generation of single photons with controlled waveform in an ion-trap cavity system," Nature **431**, 1075–1078 (2004).

[101] P. Michler, A. Kiraz, C. Becher, W. V. Schoenfeld, P. M. Petroff, L. Zhang, E. Hu, and A. Imamoglu, "A Quantum Dot Single-Photon Turnstile Device," Science **290**, 2282–2285 (2000).

[102] C. Kurtsiefer, S. Mayer, P. Zarda, and H. Weinfurter, "Stable Solid-State Source of Single Photons," Phys. Rev. Lett. **85**, 290–293 (2000).

[103] E. Knill, R. Laflamme1, and G. J. Milburn, "A scheme for efficient quantum computation with linear optics," Nature **409**, 46–52 (2001).

[104] C. Santori, D. Fattal, J. Vučković, G. S. Solomon, Y. Yamamoto,"Indistinguishable Photons from a Single-Photon Device," Nature **419**, 594–597 (2002).

[105] T. Legero, T. Wilk, M. Hennrich, G. Rempe, A. Kuhn, "Quantum Beat of Two Single Photons," Phys Rev. Lett. **93**, 070503 (2004).

[106] A. Kiraz, M. Ehrl, Th. Hellerer, O. E. Müstecaplıoğlu, C. Bräuchle, and A. Zumbusch, "Indistinguishable Photons from a Single Molecule," Phys. Rev. Lett. **94**, 223602 (2005).

[107] J. Beugnon, M. P. A. Jones, J. Dingjan, B. Darquié, G. Messin, A. Browaeys, and P. Grangier, "Quantum Interference between Two Single Photons Emitted by Independently Trapped Atoms," Nature **440**, 779–782 (2006).

[108] P. Maunz, D. L. Moehring, S. Olmschenk, K. C. Younge, D. N. Matsukevich, and C. Monroe, "Quantum Interference of Photon Pairs from Two Remote Trapped Atomic Ions," Nature Phys **3**, 538–541 (2007).

[109] K. Sanaka, A. Pawlis, T. D. Ladd, K. Lischka, and Y. Yamamoto, "Indistinguishable Photons from Independent Semiconductor Nanostructures," Phys. Rev. Lett. **103**, 053601 (2009).

[110] B. Lounis, and M Orrit, "Single-photon sources," Reg. Prog. Phys. **68**, 1129–1179 (2005).

[111] R. Hanbury Brown and R. Q. Twiss, "Correlation between photons in two coherent beams of light," Nature **177**, 27–29 (1957).

[112] W. E. Moerner and L. Kado, "Optical detection and spectroscopy of single-molecules in solids," Phys. Rev. Lett. **62**, 2535–2538 (1989).

[113] M. Orrit and J. Bernard, "Single pentacene molecules detected by fluorescence excitation in a *p*-terphenyl crystal," Phys. Rev. Lett. **65**, 2716–2719 (1990).

[114] A.-M. Boiron, B. Lounis, and M. Orrit, "Single molecules of dibenzanthanthrene in n-hexadecane," J. Chem. Phys. **105**, 3969-3974 (1996).

[115] G. Wrigge, I. Gerhardt, J. Hwang, G. Zumhofen, and V. Sandoghdar, "Efficient coupling of photons to a single molecule and the observation of its resonance fluorescence," Nature Phys. **4**, 60-66 (2008).

[116] J. R. Lakowicz , "Principles of Fluorescence spectroscopy," 3rd ed., Springer 2006, 954 p., ISBN 0-387-31278-1.

[117] F. Träger, "Handbook of Lasers and Optics," 7th ed. Springer 2007, 1332 p., ISBN 0-387-95579-8.